広島大学学位請求論文

Phenomenology for the Lepton Flavor Mixing
(レプトン世代混合の現象論)

博士後期課程3年
広島大学大学院理学研究科
物理科学専攻

髙木　堅太

Phenomenology for the Lepton Flavor Mixing

Kenta Takagi

Graduate School of Science, Hiroshima University
Higashi-Hiroshima 739-8526, Japan

2nd March 2020

A Ph.D thesis submitted to *Hiroshima University*.

Abstract

We discuss the lepton flavor mixing and present some phenomenological approaches for this. The standard model of particle theory must be improved since we have confirmed finite mass of neutrinos by the neutrino oscillation experiments. The improved theory should explain the results of the neutrino oscillation parameters as well as the neutrino masses. We present the typical three approaches, flavor symmetry, texture zeros and modular symmetry by use of our models. We also perform numerical simulations in order to show their testability in the neutrino oscillation experiments.

* * *

This thesis is based on the following publications:

- *Revisiting A_4 model for leptons in light of NuFIT 3.2*
  S. K. Kang, Y. Shimizu, K. Takagi, S. Takahashi and M. Tanimoto
  PTEP **2018** (2018) no.8, 083B01, [arXiv:1804.10468 [hep-ph]].

- *Towards the minimal seesaw model via CP violation of neutrinos*
  Y. Shimizu, K. Takagi and M. Tanimoto
  JHEP **1711** (2017) 201, [arXiv:1709.02136 [hep-ph]]

- *Modular A_4 invariance and neutrino mixing*
  T. Kobayashi, N. Omoto, Y. Shimizu, K. Takagi, M. Tanimoto and T. H. Tatsuishi
  JHEP **1811** (2018) 196, [arXiv:1808.03012 [hep-ph]]

We also refer the following publications and preprint partially:

- *Neutrino CP violation and sign of baryon asymmetry in the minimal seesaw model*
  Y. Shimizu, K. Takagi and M. Tanimoto
  Phys. Lett. B **778** (2018) 6, [arXiv:1711.03863 [hep-ph]]

- *A_4 lepton flavor model and modulus stabilization from S_4 modular symmetry*
  T. Kobayashi, Y. Shimizu, K. Takagi, M. Tanimoto and T. H. Tatsuishi
  Phys. Rev. D **100** (2019) no.11, 115045, [arXiv:1909.05139 [hep-ph]]

Contents

Chapter 1

Introduction

1.1 Motivation

The standard model (SM) of particle physics gives many predictions and they are confirmed to be consistent with various experiments precisely. All the particles given from the SM have been discovered including Higgs particle. However, the SM is not perfect and must be improved in order to address the unsolved problems, for examples:

- The SM does not include gravity
- The SM predicts vanishing neutrino mass
- The SM has no dark matter candidate
- etc.

Our discussion is closely related to the second: the neutrino mass. The neutrino mass was found to be nonzero by the observations of neutrino oscillation which is induced by a mixing of three classes (flavors) of leptons. The lepton mixing of three flavors is described by the Pontecorvo–Maki–Nakagawa–Sakata (PMNS) matrix, a 3×3 unitary matrix [1, 2]. A theoretical approach to the finite neutrino mass must be consistent to the neutrino oscillation experiments. The current neutrino oscillation experiments have shown two large mixing alngles $\theta_{12} \simeq 33.8^\circ$, $\theta_{23} \simeq 48.3^\circ$ and one small mixing angle $\theta_{13} \simeq 8.61^\circ$ [3] which parametrize the PMNS matrix. It is also important that T2K [4, 5] and NOνA [6, 7] experiments strongly indicate the CP violation in the flavor mixing. The precision of neutrino oscillation experiments is expected to be improved in the future. We shall present three approaches to the lepton flavor mixing and show their predictions which will be expected to be testable in the future experiments.

An interesting approach is to assume the flavor symmetry as the origin of flavors by use of non-Abelian discrete groups (see [8–16] for useful review articles.) One can find models of flavor symmetry with S_3 in Refs. [17, 18] for quark mixing and [19, 20] for lepton mixing. The A_4 models appear in Refs. [21–27]. One can also find S_4 [28], A_5 [29], $\Delta(27)$ [30] models and larger groups. They introduce several SU(2) gauge singlet scalar fields called as flavons. The Yukawa coupling constants are determined by the vacuum expectation values (VEVs) of flavons at the flavor symmetry breaking, which can explain the results of neutrino oscillation experiments. We will discuss a model of the flavor symmetry of A_4 based on [27].

There are so many candidates of flavor symmetry that it is difficult to specify the correct model even if the experimental data determine the whole mixing parameters. We should make a minimal model in order to obtain a testable prediction since we have only five observables which constrain our model: the three lepton mixing angles and two mass squared differences. A top-down approach based on the experimental results are important to find a minimal model [31–48], which does not specify a flavor symmetry. We impose zeros in the mass matrix of the charged leptons and/or neutrino mass matrix, and such approach is often called as the texture zeros. We study a minimal model [47] where two light-handed neutrinos are introduced. We will see the sharp predictions for the Dirac CP violating phase up to its sign.

There is an attractive method to obtain S_3, A_4, S_4 and A_5 groups as quotient groups of the modular group [49]. The modular symmetry is realized in the torus compactification as well as the orbifold compactification of extra dimensions. Superstring theory predicts six-dimensional compact space in addition to four-dimensional space-time. We consider the modular symmetry obtained from the six-dimensional compact space and make a flavor symmetric model. An interesting ansatz was proposed for $\Gamma_3 \simeq A_4$ modular symmetry in Ref. [50] where Yukawa couplings behave as holomorphic functions of the modulus τ (a complex parameter) and transform as A_4 triplet representations, and they are called the modular forms. The value of τ is determined at the modular symmetry breaking: at the Planck scale or slightly above. Such a model can be built with smaller number of free parameters than an ordinary flavor symmetric model since the modular forms can play the same role as flavons by given τ. A numerical discussion for two specific models with $\Gamma_3 \simeq A_4$ can be seen in [51]. Among them, our paper based on Ref. [52] performs further numerical discussions in order to show a clear testability for the relevant experiments.

One can find modular forms of weight 2 which transforms as representations of S_3 [53], S_4 [54], A_5 [55], $\Delta(96)$, and $\Delta(384)$ [56]. It will be useful to refer a textbook of the modular forms [58]. The modular forms of the weight 1 and higher odd weights are also shown for a double covering group T' doublet [57]. The modular symmetric models have been studied for the flavors by use of these modular forms [50–52, 59–85].

We discuss the phenomenological aspects of the model:

- Dirac CP violating phases and flavor mixing
- The neutrino masses
- The effective neutrino mass of the neutrinoless double beta decay
- Majorana CP violating phases

1.2 Overview the phenomenological targets

We overview the phenomenological aspects featured in our present model. We show the flavor mixing of the fermions and some mechanism to obtain finite neutrino masses. We also show a phenomenological indication of Majorana neutrinos, which may give strong candidates to explain the small neutrino masses.

1.2.1 Flavor mixing in the SM

We briefly review the flavor mixing in the SM. The SM has three flavors for the fermions. The flavor mixing is described by a 3×3 unitary matrix which connects the two different basis of the fermions. The flavor eigenstates appear in the Lagrangian. The mass eigenstates are another basis written in terms of their mass eigenvalues.

Let us define the flavor eigenstates of the SM fermions. The left- and right-handed fermions are described separately as SU(2) doublets and singlets respectively:

$$\boldsymbol{q}_L = \begin{pmatrix} \boldsymbol{u}_L \\ \boldsymbol{d}_L \end{pmatrix}, \quad \boldsymbol{l}_L = \begin{pmatrix} \boldsymbol{\nu}_L \\ \boldsymbol{e}_L \end{pmatrix}, \quad \boldsymbol{u}_R, \quad \boldsymbol{d}_R, \quad \boldsymbol{e}_R, \tag{1.2.1}$$

where the left-handed quark doublet $\boldsymbol{q}_L$ is composed by up- and down-type quarks: $\boldsymbol{u}_L$ and $\boldsymbol{d}_L$; and the left-handed lepton doublet $\boldsymbol{l}_L$ includes neutrinos and charged leptons: $\boldsymbol{\nu}_L$ and $\boldsymbol{e}_L$. The right-handed up-type quarks, down-type quarks and the charged leptons are denoted by $\boldsymbol{u}_R$, $\boldsymbol{d}_R$ and $\boldsymbol{e}_R$ respectively. Those fermion fields includes three flavors named as:

$$\begin{aligned}
&\boldsymbol{u}_L = (u_L, c_L, t_L)^T, \quad \boldsymbol{d}_L = (d_L, s_L, b_L)^T, \\
&\boldsymbol{e}_L = (e_L, \mu_L, \tau_L)^T, \quad \boldsymbol{\nu}_L = (\nu_e, \nu_\mu, \nu_\tau)^T \\
&\boldsymbol{u}_R = (u_R, c_R, t_R)^T, \quad \boldsymbol{d}_R = (d_R, s_R, b_R)^T, \quad \boldsymbol{e}_R = (e_R, \mu_R, \tau_R)^T.
\end{aligned} \tag{1.2.2}$$

Those left- and right-handed fields are massless. We can write the Yukawa interaction with these left- and right-handed fermion fields and the Higgs scalar field Φ:

$$\mathcal{L}_{yuk} = y_u^{ij} \bar{\boldsymbol{u}}_R^i \tilde{\Phi} \boldsymbol{q}_L^j + y_d^{ij} \bar{\boldsymbol{d}}_R^i \Phi \boldsymbol{q}_L^j + y_e^{ij} \bar{\boldsymbol{e}}_R^i \Phi \boldsymbol{l}_L^j + \text{h.c.}, \tag{1.2.3}$$

where the Higgs fields is a SU(2) doublet:

$$\Phi = \begin{pmatrix} \varphi^+ \\ \varphi^0 \end{pmatrix}, \tag{1.2.4}$$

and $\tilde{\Phi} = i\tau_2 \Phi^*$. The coupling constants y_u^{ij}, y_d^{ij} and y_e^{ij} are complex 3×3 matrices of flavor space in general. The spontaneous symmetry breaking of the Higgs field $\langle \Phi \rangle = (0, v/\sqrt{2})^T$ induces finite masses for the ferminons:

$$M_u^{ij} = \frac{v}{\sqrt{2}} y_u^{ij}, \quad M_d^{ij} = \frac{v}{\sqrt{2}} y_d^{ij}, \quad M_e^{ij} = \frac{v}{\sqrt{2}} y_e^{ij}, \tag{1.2.5}$$

where $v = 246$ [GeV]. We can always change the basis into the mass basis where the fermion mass matrices are diagonal:

$$\begin{aligned}
M_u^{diag} &= \text{diag}\,[m_u, m_c, m_t], \\
M_d^{diag} &= \text{diag}\,[m_d, m_s, m_b], \\
M_e^{diag} &= \text{diag}\,[m_e, m_\mu, m_\tau],
\end{aligned} \tag{1.2.6}$$

by unitary transformations. The mass matrices are diagonalized by the following unitary transformation:

$$M_u^{diag} = U_R^u M_u U_L^{u\dagger}, \quad M_d^{diag} = U_R^d M_d U_L^{d\dagger}, \quad M_e^{diag} = U_R^{e\dagger} M_e U_L^e. \tag{1.2.7}$$

We redefine the fermion fields except the neutrinos as

$$\begin{aligned} \boldsymbol{u}'_L &\equiv U_L^u \boldsymbol{u}_L, \quad \boldsymbol{d}'_L \equiv U_L^d \boldsymbol{d}_L, \quad \boldsymbol{e}'_L \equiv U_L^{e\dagger} \boldsymbol{e}_L, \\ \boldsymbol{u}'_R &\equiv U_R^u \boldsymbol{u}_R, \quad \boldsymbol{d}'_R \equiv U_R^d \boldsymbol{d}_R, \quad \boldsymbol{e}'_R \equiv U_R^{e\dagger} \boldsymbol{e}_R. \end{aligned} \tag{1.2.8}$$

We call these redefined fields as the mass eigenstates.

Let's consider the charged weak current of the quark sector and the interchange of the flavor/mass basis.

$$J_q^\mu = \bar{\boldsymbol{u}}_L \gamma^\mu \boldsymbol{d}_L = \bar{\boldsymbol{u}}'_L \gamma^\mu (U_L^u U_L^{d\dagger}) \boldsymbol{d}'_L. \tag{1.2.9}$$

The quark flavor mixing, Cabibbo–Kobayashi–Maskawa (CKM) matrix [86,87], is defined as:

$$V_{CKM} \equiv U_L^u U_L^{d\dagger}. \tag{1.2.10}$$

We can also define the lepton mixing in the charged weak current:

$$J_e^\mu = \bar{\boldsymbol{\nu}}_L \gamma^\mu \boldsymbol{e}_L = \bar{\boldsymbol{\nu}}'_L (U_L^{e\dagger} U_L^\nu)^\dagger \gamma^\mu \boldsymbol{e}'_L, \tag{1.2.11}$$

where we have introduced a unitary matrix U_L^ν and a new basis of the neutrino fields $\boldsymbol{\nu}'_L$. Although we cannot obtain the finite neutrino masses due to the absence of right-handed neutrinos in the SM, we call the new basis $\boldsymbol{\nu}'_L$ the mass basis of neutrino fields and it is defined as

$$\boldsymbol{\nu}'_L \equiv U_L^{\nu\dagger} \boldsymbol{\nu}_L. \tag{1.2.12}$$

The unitary matrix $U_L^{\nu\dagger}$ should be determined by diagonalization of the neutrino mass matrix obtained from some mechanism beyond the SM. We emphasize that the evidence of finite neutrino masses were discovered in the neutrino oscillation experiment at Super-Kamiokande (1998) [88]. The lepton mixing matrix is defined as

$$U_{PMNS} = U_L^{e\dagger} U_L^\nu, \tag{1.2.13}$$

which is called Pontecorvo–Maki–Nakagawa–Sakata (PMNS) matrix [1,2].

We have some degrees of freedom to parametrize the CKM and PMNS matrices. We employ the Particle Data Group (PDG) convention [89] in this thesis. The CKM matrix is parametrized by 2-3, 1-3 and 1-2 plane rotation matrices:

$$\begin{aligned} V_{CKM} &= \begin{pmatrix} 1 & 0 & 0 \\ 0 & c_{23} & s_{23} \\ 0 & -s_{23} & c_{23} \end{pmatrix} \begin{pmatrix} c_{13} & 0 & s_{13} e^{-i\delta_{CP}^q} \\ 0 & 1 & 0 \\ -s_{13} e^{i\delta_{CP}^q} & 0 & c_{13} \end{pmatrix} \begin{pmatrix} c_{12} & s_{12} & 0 \\ -s_{12} & c_{12} & 0 \\ 0 & 0 & 1 \end{pmatrix} \\ &= \begin{pmatrix} c_{12} c_{13} & s_{12} c_{13} & s_{13} e^{-i\delta_{CP}^q} \\ -s_{12} c_{23} - c_{12} s_{23} s_{13} e^{i\delta_{CP}^q} & c_{12} c_{23} - s_{12} s_{23} s_{13} e^{i\delta_{CP}^q} & s_{23} c_{13} \\ s_{12} s_{23} - c_{12} c_{23} s_{13} e^{i\delta_{CP}^q} & -c_{12} s_{23} - s_{12} c_{23} s_{13} e^{i\delta_{CP}^q} & c_{23} c_{13} \end{pmatrix}, \end{aligned} \tag{1.2.14}$$

where c_{ij} and s_{ij} denote $\cos\theta_{ij}$ and $\sin\theta_{ij}$, respectively. The Dirac CP violating phase δ^q_{CP} cannot be absorbed in redefinition of the fermion fields. The PMNS matrix is parametrized as

$$U_{PMNS} = \begin{pmatrix} c_{12}c_{13} & s_{12}c_{13} & s_{13}e^{-i\delta^l_{CP}} \\ -s_{12}c_{23} - c_{12}s_{23}s_{13}e^{i\delta^l_{CP}} & c_{12}c_{23} - s_{12}s_{23}s_{13}e^{i\delta^l_{CP}} & s_{23}c_{13} \\ s_{12}s_{23} - c_{12}c_{23}s_{13}e^{i\delta^l_{CP}} & -c_{12}s_{23} - s_{12}c_{23}s_{13}e^{i\delta^l_{CP}} & c_{23}c_{13} \end{pmatrix} P, \quad (1.2.15)$$

with $P = \mathrm{diag}\,[1, e^{i\alpha_{21}/2}, e^{i\alpha_{31}/2}]$. The Dirac CP violating phase is denoted as δ^l_{CP}. The Majorana CP violating phases are α_{21} and α_{31}, which are defined if the neutrinos are Majorana particles.

We obtain the three lepton mixing angles in terms of the PMNS matrix elements of the PDG parametrization as

$$\sin^2\theta_{12} = \frac{|U_{e2}|^2}{1-|U_{e3}|^2}\ , \quad \sin^2\theta_{23} = \frac{|U_{\mu 3}|^2}{1-|U_{e3}|^2}\ , \quad \sin^2\theta_{13} = |U_{e3}|^2, \quad (1.2.16)$$

where $U_{\alpha i}$ is the PMNS matrix elements. We also have the Dirac CP violating phase δ_{CP}:

$$\sin\delta_{CP} = \frac{J_{CP}}{s_{23}c_{23}s_{12}c_{12}s_{13}c_{13}^2}, \quad (1.2.17)$$

where J_{CP} is a measure of the CP violation called as the Jarlskog invariant [92]:

$$J_{CP} = \mathrm{Im}\left[U_{e1}U_{\mu 2}U^*_{\mu 1}U^*_{e2}\right]. \quad (1.2.18)$$

The current global fit of the two mass squared differences and three mixing angles given by NuFIT 4.2 (2019) [3] is shown in Tab. 1.2.1.

observable	$3\,\sigma$ C.L. for NH	$3\,\sigma$ C.L. for IH
$\Delta m^2_{\mathrm{atm}}$	$(2.436 - 2.618) \times 10^{-3}\mathrm{eV}^2$	$-(2.419–2.601) \times 10^{-3}\mathrm{eV}^2$
$\Delta m^2_{\mathrm{sol}}$	$(6.79 - 8.01) \times 10^{-5}\mathrm{eV}^2$	$(6.79 - 8.01) \times 10^{-5}\mathrm{eV}^2$
$\sin^2\theta_{12}$	$0.275 - 0.350$	$0.275 - 0.350$
$\sin^2\theta_{23}$	$0.433 - 0.609$	$0.436 - 0.610$
$\sin^2\theta_{13}$	$0.02044 - 0.02435$	$0.02064 - 0.02457$

Table 1.2.1: The global fit of the neutrino oscillation experiments from NuFIT 4.1 in $3\,\sigma$ C.L. [3]. We use $\Delta m^2_{\mathrm{sol}} \equiv m_2^2 - m_1^2$; and we use $\Delta m^2_{\mathrm{atm}} \equiv m_3^2 - m_1^2$ or $m_3^2 - m_2^2$ for NH or IH respectively.

1.2.2 Neutrino mass

The neutrino experiments indicates finite neutrino masses. We can access only the mass squared differences from the neutrino oscillation denoted as $\Delta m^2_{21} \equiv m_2^2 - m_1^2$ and $\Delta m^2_{31} \equiv m_3^2 - m_1^2$ with the notation of

$$\mathrm{diag}\,[m_1, m_2, m_3] \equiv U^{\nu\dagger}_R M_\nu U^\nu_L, \quad (1.2.19)$$

where m_1, m_2 and m_3 are real eigenvalues of the neutrino mass matrix. We have two possibilities of the neutrino mass hierarchy since the sign of Δm_{31}^2 is still unknown and Δm_{21}^2 is found to be positive:

$$\begin{cases} m_1 < m_2 \ll m_3 & \text{Normal Hierarchy (NH)} \\ m_3 \ll m_1 < m_2 & \text{Inverted Hierarchy (IH)} \end{cases}, \tag{1.2.20}$$

In the theory, there are two ways to obtain mass terms for the fermions: The first is the couplings between left- and right-handed particles as seen in Eq.(1.2.3). If we have the right-handed neutrinos in addition to the SM, we obtain the Dirac mass term

$$y_{ij}^{\nu} \bar{\boldsymbol{\nu}}_R^i \tilde{\Phi} \boldsymbol{\nu}_L^j + \text{h.c.}. \tag{1.2.21}$$

However, it seems difficult to give a natural explanation why the mass of neutrino is much smaller than that of the other charged particles. We need some mechanism to induce small masses for the neutrinos even if we introduce the right-handed neutrinos. The second is the Majorana mass term:

$$M_\nu (\bar{\boldsymbol{\nu}}_L^c \boldsymbol{\nu}_L + \text{h.c.}), \tag{1.2.22}$$

where $\bar{\boldsymbol{\nu}}_L^c$ denotes the charge conjugation of $\bar{\boldsymbol{\nu}}_L$ and has the right-handed chirality. In the following, we assume the neutrinos are Majorana particles to explain small neutrino masses.

Weinberg operator

We explain small masses of the neutrinos without introducing right-handed neutrinos. The Majorana mass term Eq.(1.2.22) is derived from the following 5 dimensional operator:

$$y^\nu \bar{\boldsymbol{l}}_L^c \boldsymbol{l}_L \Phi\Phi \frac{1}{\Lambda}, \tag{1.2.23}$$

which is called the Weinberg operator [90]. The constant Λ is the cut off scale which corresponds to some physical energy scale. We have a symmetric mass matrix of the neutrinos by the electro-weak symmetry breaking:

$$M_\nu = \frac{v^2}{2\Lambda} y_\nu. \tag{1.2.24}$$

If the Yukawa coupling matrix is $\mathcal{O}(1)$, $M_\nu \sim 3$ meV for the GUT scale ($\Lambda \sim 10^{16}$ GeV).

Type I seesaw mechanism

We have another way to obtain the mass term Eq.(1.2.23) effectively by introducing right-handed Majorana neutrinos $\boldsymbol{\nu}_R$ which are SU(2) gauge singlet fermions [91]. The neutrino mass terms can be described as

$$\mathcal{L} = (y_D \bar{\boldsymbol{\nu}}_R \tilde{\Phi} \boldsymbol{\nu}_L + \text{h.c.}) - \frac{1}{2} M_N \bar{\boldsymbol{\nu}}_R^c \boldsymbol{\nu}_R, \tag{1.2.25}$$

where the Majorana neutrino mass matrix M_N is a symmetric matrix. If the right-handed neutrinos have heavy mass ($M_N \gg \langle\Phi\rangle$), the masses of the left-handed neutrinos are relatively very small in this Lagrangian. The effective left-handed neutrino mass term can be written by integrating out the heavy right-handed neutrino fields, which corresponds to the Weinberg operator Eq. (1.2.23). The effective mass matrix of left-handed neutrinos are obtained as a mixing of the left- and right-handed sectors:

$$M_\nu = -M_D^T (M_N)^{-1} M_D, \tag{1.2.26}$$

where M_D is the Dirac mass term $M_D = y_D\langle\Phi\rangle$. The small neutrino mass is explained through the above mixing with heavy right-handed neutrinos, which is called the seesaw mechanism.

The neutrino mass matrix is symmetric for both Weinberg operator case and type I seesaw case. We note that a general symmetric matrix S can be diagonalized with a unitary matrix U as $U^T SU$. A Hermitian matrix H can be diagonalized by $V^\dagger HV$ with a unitary matrix V.

1.2.3 Neutrinoless double beta decay

If the neutrinos are Majorana particles, we can find a signal of the neutrinoless double beta decay ($0\nu\beta\beta$). The well known beta decay of neutron is written as

$$n \longrightarrow p + e^- + \bar{\nu}_e \tag{1.2.27}$$

If the neutrinos are Majorana particles the following $0\nu\beta\beta$ process is expected in a nucleus:

$$2n \longrightarrow 2p + 2e^+ \tag{1.2.28}$$

with annihilation of a $\bar{\nu}_e$ pair since a neutrino and anti-neutrino are identical. Its amplitudes can be obtained from the interaction between two electro-weak charged currents $e^- \to W^-\bar{\nu}_L$. It is proportional to the effective mass of ν_e as

$$\mathcal{A} \propto \langle m_{ee}\rangle, \quad \langle m_{ee}\rangle \equiv \sum_i^3 m_i U_{ei}^2 \tag{1.2.29}$$

where m_i denotes the mass eigenvalue of the neutrinos and U_{ei} denotes a element of the PMNS matrix. The KamLAND-Zen collaboration [95] provides the upper bound for $\langle m_{ee}\rangle$ reported as

$$\langle m_{ee}\rangle < [0.061, 0.165]\,\text{eV}. \tag{1.2.30}$$

Chapter 2

Flavor symmetry

We discuss the origin of the flavor structure. The neutrino oscillation experiments revealed that the lepton mixing is quite different from the quark mixing:

$$V_{CKM} \sim \begin{pmatrix} 0.97446 & 0.22452 & 0.00365 \\ 0.22438 & 0.97359 & 0.04214 \\ 0.00896 & 0.04133 & 0.99911 \end{pmatrix}, \quad U_{PMNS} \sim \begin{pmatrix} 0.82 & 0.55 & 0.15 \\ 0.30 & 0.70 & 0.74 \\ 0.50 & 0.58 & 0.65 \end{pmatrix}, \tag{2.0.1}$$

which are obtained from the best fit value of PDG (2018) [89] for CKM mixing and NuFIT 4.1 (2019) [3] for PMNS mixing. One can find that the two mixing matrices are quite different: V_{CKM} is almost a unit matrix and U_{PMNS} is a large mixing. Before 2012, when a non-vanishing value of θ_{13} in the lepton mixing was discovered, the experimental results of the neutrino oscillation seemed to be consistent with an interesting structure:

$$U_{TBM} = \begin{pmatrix} \sqrt{2/3} & \sqrt{1/3} & 0 \\ -\sqrt{1/6} & \sqrt{1/3} & -\sqrt{1/2} \\ -\sqrt{1/6} & \sqrt{1/3} & \sqrt{1/2} \end{pmatrix}, \tag{2.0.2}$$

which is called the tri-bimaximal mixing (TBM) [93, 94]. A lot of models were presented to obtain the origin of flavor structure with new symmetry G in addition to SM inspired by the TBM. The new symmetry G is set in the three flavors and called as the flavor symmetry. The TBM structure was theoretically obtained by a non-Abelian discrete group $G = A_4$ [23, 24]. It is remarked that non-zero value of θ_{13} was predicted by a flavor symmetric model before 2012 [25]. The flavor symmetry is therefore still a powerful tool to investigate the origin of flavor and we can find many flavor models by means of S_3, A_4, S_4, A_5 and other groups with larger orders [17–30].

The recent neutrino oscillation experiments have been developed and strongly indicates the CP violation $\delta^l_{CP} \neq 0, \pm\pi$ as well as the non-zero θ_{13}. The future experimental development will require models with sharper and more detailed predictions.

2.1 Model with flavor symmetry

The flavor symmetry is a powerful tool to obtain a sharp prediction for the neutrino experiments. We show a model of flavor symmetry with a non-Abelian discrete group A_4

	L	e_R, μ_R, τ_R	h_u	h_d	ϕ_T	η	$\tilde{\eta}$	ϕ_S	ξ	$\tilde{\xi}$	Θ
$SU(2)$	2	1	2	2	1	1	1	1	1	1	1
A_4	3	1, $1''$, $1'$	1	1	3	$1''$	$1''$	3	a	a	a
Z_3	ω	ω^2	1	1	1	1	1	ω	ω	ω	1
$U(1)_{FN}$	0	4, 2, 0	0	0	0	0	0	0	0	0	-1
$U(1)_R$	1	1	0	0	0	0	0	0	0	0	0

Table 2.1.1: The charge assignment for the fermions, Higgs fields and flavons where $\omega = \exp[2\pi i/3]$.

and Z_3 [27]. The theory is described in supersymmetric theory in order to achieve the potential analysis of the flavons.

2.1.1 Set up

We have to introduce two Higgs doublets, h_u and h_d, in order to prevent the triangle anomaly in supersymmetry and they are supposed to be trivial singlets of A_4. There are several SU(2) gauge singlet scalar fields denoted as ϕ_T, η, $\tilde{\eta}$, ϕ_S, ξ and $\tilde{\xi}$. We have the required neutrino and charged lepton masses by the specific VEVs in the Yukawa coupling. The additional symmetries A_4, Z_3 and $U(1)_{FN}$ control the Yukawa couplings involved by the flavons. A specific charge assignment can also prohibit unwanted couplings in the Lagrangian. In particular, the Froggatt–Nielsen (FN) mechanism [96] realizes the hierarchical masses of the charged leptons m_e, m_μ and m_τ with the FN flavon Θ and appropriate FN charge $U(1)_{FN}$. The $U(1)_R$ symmetry is necessary to prevent dangerous proton decay channels.

The charge assignment of the fermions and flavons are summarized in Tab. 2.1.1 It is noted that the theory does not contain a right-handed neutrinos.

The global transformations of A_4 are given by the generators S and T which are summarized in Eq. (A.0.1) for the A_4 representations of $\mathbf{1}$, $\mathbf{1}'$, $\mathbf{1}''$ and $\mathbf{3}$. The Z_3 transformation gives rise to $\omega = \exp[2\pi i/3]$ or ω^2 factor. The global $U(1)_{FN}$ and $U(1)_R$ transformation yields $\exp[i\theta_{FN}]$ and $\exp[i\theta_R]$ up to the order of its charge. The invariant theory is realized when each coupling gives trivial transformation in the superpotential except for $U(1)_R$. We must impose the $U(1)_R$ charge 2 to the superpotential for invariance.

2.1.2 Yukawa couplings

We have a superpotential of the Yukawa couplings:

$$w = w_l + w_\nu \tag{2.1.1}$$

where w_l and w_ν denotes the charged lepton sector and neutrino sector respectively. The $A_4 \otimes Z_3 \otimes U(1)_{FN} \otimes U(1)_R$ symmetry is realized by the following charged lepton mass

	ϕ_0^T	η_0	ϕ_0^S	ξ_0
$SU(2)$	1	1	1	1
A_4	3	1	3	1
Z_3	1	ω^2	ω	ω
$U(1)_{FN}$	0	0	0	0
$U(1)_R$	2	2	2	2

Table 2.1.2: The charge assignment for the driving fields.

term:

$$\begin{aligned} w_l &= y_e\,(\phi_T l)_{\mathbf{1}}\, e^c h_d \frac{\Theta^4}{\Lambda^5} + y_\mu\,(\phi_T l)_{\mathbf{1}'}\, \mu^c h_d \frac{\Theta^2}{\Lambda^3} + y_\tau\,(\phi_T l)_{\mathbf{1}''}\, \tau^c h_d \frac{1}{\Lambda} \\ &+ y_e'\,(\phi_T l)_{\mathbf{1}'}\, e^c h_d \frac{\eta\Theta^4}{\Lambda^6} + y_\mu'\,(\phi_T l)_{\mathbf{1}''}\, \mu^c h_d \frac{\eta\Theta^2}{\Lambda^4} + y_\tau'\,(\phi_T l)_{\mathbf{1}}\, \tau^c h_d \frac{\eta}{\Lambda^2}, \end{aligned} \tag{2.1.2}$$

and the neutrino mass term obtained by the Weinberg operator:

$$\begin{aligned} w_\nu &= y_S (ll)_{\mathbf{3}} h_u h_u \frac{\phi_S}{\Lambda^2} + y_\xi (ll)_{\mathbf{1}} h_u h_u \frac{\xi}{\Lambda^2} \\ &+ y_1'(ll)_{\mathbf{1}} h_u h_u \frac{(\phi_S\phi_T)_{\mathbf{1}}}{\Lambda^3} + y_2'(ll)_{\mathbf{1}'} h_u h_u \frac{(\phi_S\phi_T)_{\mathbf{1}''}}{\Lambda^3} \\ &+ y_3'(ll)_{\mathbf{1}''} h_u h_u \frac{(\phi_S\phi_T)_{\mathbf{1}'}}{\Lambda^3} + y_4'(ll)_{\mathbf{3}} h_u h_u \frac{(\phi_S\phi_T)_{\mathbf{3}}}{\Lambda^3} \\ &+ y_5'(ll)_{\mathbf{3}} h_u h_u \frac{\phi_S \eta}{\Lambda^3} + y_6'(ll)_{\mathbf{3}} h_u h_u \frac{\xi\phi_T}{\Lambda^3} + y_7'(ll)_{\mathbf{1}'} h_u h_u \frac{\xi\eta}{\Lambda^3}, \end{aligned} \tag{2.1.3}$$

up to the next-to-leading order where Λ is the cut-off scale. The Yukawa coupling constants ys are assumed to be order one. The charged leptons and neutrinos obtain their masses by finite VEVs of the flavons as well as Higgs scale fields.

2.1.3 Potential analysis

We also introduce additional SU(2) gauge singlet fields called as the driving fields: ϕ_0^T, η_0, ϕ_0^S and ξ_0. They are separated from the Yukawa couplings due to their $U(1)_R$ charge. The charge assignment of the driving fields is summarized in Tab. 2.1.3. We can obtain the mass terms of the flavons coupled with the driving fields:

$$w_d = w_d^T + w_d^S, \tag{2.1.4}$$

where

$$\begin{aligned} w_d^T &= -M\phi_0^T\phi_T + g\phi_0^T\phi_T\phi_T + \lambda\phi_0^T\phi_T\tilde{\eta} \\ &- \lambda_1\eta_0\phi_T\phi_S + \lambda_2\eta_0\eta\xi + \lambda_3\eta_0\eta\tilde{\xi} + \lambda_4\eta_0\tilde{\eta}\xi + \lambda_5\eta_0\tilde{\eta}\tilde{\xi} \end{aligned} \tag{2.1.5}$$

and

$$w_d^S = g_1\phi_0^S\phi_S\phi_S + g_2\phi_0^S\phi_S\tilde{\xi} - g_3\xi_0\phi_S\phi_S + g_4\xi_0\xi\xi + g_5\xi_0\xi\tilde{\xi} + g_6\xi_0\tilde{\xi}\tilde{\xi}, \tag{2.1.6}$$

where M is a complex mass parameter. The trilinear couplings gs and λs are also complex parameters of order one. It is noted that w_d^S is the same superpotential given in Ref. [24]. The multiplication rule of A_4 group in Appendix A gives the following decompositions:

$$\begin{aligned}
w_d^T &= -M\left(\phi_{01}^T\phi_{T1}+\phi_{02}^T\phi_{T3}+\phi_{03}^T\phi_{T2}\right)+\lambda\left(\phi_{01}^T\phi_{T2}+\phi_{02}^T\phi_{T1}+\phi_{03}^T\phi_{T3}\right)\tilde{\eta} \\
&+\frac{2g}{3}\left[\phi_{01}^T\left(\phi_{T1}^2-\phi_{T2}\phi_{T3}\right)+\phi_{02}^T\left(\phi_{T2}^2-\phi_{T1}\phi_{T3}\right)+\phi_{03}^T\left(\phi_{T3}^2-\phi_{T1}\phi_{T2}\right)\right] \\
&-\lambda_1\eta_0\left(\phi_{T2}\phi_{S2}+\phi_{T1}\phi_{S3}+\phi_{T3}\phi_{S1}\right)+\lambda_2\eta_0\eta\xi+\lambda_3\eta_0\eta\tilde{\xi}+\lambda_4\eta_0\tilde{\eta}\xi+\lambda_5\eta_0\tilde{\eta}\tilde{\xi}, \\
w_d^S &= \frac{2g_1}{3}\left[\phi_{01}^S\left(\phi_{S1}^2-\phi_{S2}\phi_{S3}\right)+\phi_{02}^S\left(\phi_{S2}^2-\phi_{S1}\phi_{S3}\right)+\phi_{03}^S\left(\phi_{S3}^2-\phi_{S1}\phi_{S2}\right)\right] \\
&+g_2\left(\phi_{01}^S\phi_{S1}+\phi_{02}^S\phi_{S3}+\phi_{03}^S\phi_{S2}\right)\tilde{\xi} \\
&-g_3\xi_0\left(\phi_{S1}^2+2\phi_{S2}\phi_{S3}\right)+g_4\xi_0\xi^2+g_5\xi_0\xi\tilde{\xi}+g_6\xi_0\tilde{\xi}^2,
\end{aligned} \tag{2.1.7}$$

Note that we have new terms relevant to η and $\tilde{\eta}$ in addition to w_d^T appeared in Ref. [24]. In $N=1$ global SUSY, the scalar potential of the F-term is given by the superpotential as

$$V=\sum_i\left|\frac{\partial w}{\partial\phi_i}\right|^2+\text{h.c.}, \tag{2.1.8}$$

where ϕ_i is a chiral superfield in the superpotential w. The relevant scalar potential $V=V_T+V_S$ is given by

$$\begin{aligned}
V_T &= \sum_i\left|\frac{\partial w_d^T}{\partial\phi_{0i}^T}\right|^2+\text{h.c.} \\
&= 2\left|-M\phi_{T1}+\lambda\phi_{T2}\tilde{\eta}+\frac{2g}{3}\left(\phi_{T1}^2-\phi_{T2}\phi_{T3}\right)\right|^2 \\
&+2\left|-M\phi_{T3}+\lambda\phi_{T1}\tilde{\eta}+\frac{2g}{3}\left(\phi_{T2}^2-\phi_{T1}\phi_{T3}\right)\right|^2 \\
&+2\left|-M\phi_{T2}+\lambda\phi_{T3}\tilde{\eta}+\frac{2g}{3}\left(\phi_{T3}^2-\phi_{T1}\phi_{T2}\right)\right|^2 \\
&+2\left|-\lambda_1\left(\phi_{T2}\phi_{S2}+\phi_{T1}\phi_{S3}+\phi_{T3}\phi_{S1}\right)+\lambda_2\eta\xi+\lambda_3\eta\tilde{\xi}+\lambda_4\tilde{\eta}\xi+\lambda_5\tilde{\eta}\tilde{\xi}\right|^2, \\
V_S &= \sum\left|\frac{\partial w_d^S}{\partial X}\right|^2+\text{h.c.} \\
&= 2\left|\frac{2g_1}{3}\left(\phi_{S1}^2-\phi_{S2}\phi_{S3}\right)+g_2\phi_{S1}\tilde{\xi}\right|^2+2\left|\frac{2g_1}{3}\left(\phi_{S2}^2-\phi_{S1}\phi_{S3}\right)+g_2\phi_{S3}\tilde{\xi}\right|^2 \\
&+2\left|\frac{2g_1}{3}\left(\phi_{S3}^2-\phi_{S1}\phi_{S2}\right)+g_2\phi_{S2}\tilde{\xi}\right|^2 \\
&+2\left|-g_3\left(\phi_{S1}^2+2\phi_{S2}\phi_{S3}\right)+g_4\xi^2+g_5\xi\tilde{\xi}+g_6\tilde{\xi}^2\right|^2.
\end{aligned} \tag{2.1.9}$$

We find the potential minimum $V_T = 0$ and $V_S = 0$ at the following VEVs

$$\begin{aligned}
\langle\phi_T\rangle =& v_T \begin{pmatrix}1\\0\\0\end{pmatrix}, \quad \langle\phi_S\rangle = v_S \begin{pmatrix}1\\1\\1\end{pmatrix}, \quad \langle\eta\rangle = q, \quad \langle\tilde{\eta}\rangle = 0, \quad \langle\xi\rangle = u, \quad \langle\tilde{\xi}\rangle = 0, \\
v_T =& \frac{3M}{2g}, \qquad v_S^2 = \frac{g_4}{3g_3}u^2, \qquad q = \frac{\lambda_1 v_T v_S}{\lambda_2 u} = \frac{\lambda_1}{\lambda_2}\sqrt{\frac{g_4}{3g_3}} v_T \ ,
\end{aligned} \tag{2.1.10}$$

where we take the VEVs of $\tilde{\xi}$ and $\tilde{\eta}$ to be zero in the linear transformation between ξ and $\tilde{\xi}$ as well as η and $\tilde{\eta}$. We can obtain the nonzero VEV of Θ from the scalar potential of D-term if we assume a gauged $U(1)_{\rm FN}$. The Fayet-Iliopolos term gives the finite VEV of Θ [97]. Thus, The VEVs of v_T, v_S, u and q are the independent free parameters of the model.

2.1.4 Mass matrix

We write the mass matrices of the charged leptons and neutrinos with the VEVs of Eq.(2.1.10) as well as the Higgs fields: $\langle H_u\rangle = v_u$ and $\langle H_d\rangle = v_d$. The lepton mass matrices are constructed from the superpotentials w_l in Eq. (2.1.2) and w_ν in Eq. (2.1.3). These superpotentials are decomposed according to the multiplication rule of A_4 given in Appendix A.

Charged lepton mass matrix

The charged lepton mass matrix is written as:

$$M_\ell = v_d\alpha_\ell \begin{pmatrix} y_e\lambda^4 & 0 & y'_\tau\alpha_\eta \\ y'_e\alpha_\eta\lambda^4 & y_\mu\lambda^2 & 0 \\ 0 & y'_\mu\alpha_\eta\lambda^2 & y_\tau \end{pmatrix} \tag{2.1.11}$$

where the parameters α_ℓ, α_η and λ are written in terms of the VEVs of ϕ_T, η and Θ, respectively:

$$\alpha_\ell \equiv \frac{\langle\phi_T\rangle}{\Lambda} = \frac{v_T}{\Lambda} \ , \qquad \alpha_\eta \equiv \frac{\langle\eta\rangle}{\Lambda} = \frac{q}{\Lambda} \ , \qquad \lambda \equiv \frac{\langle\Theta\rangle}{\Lambda} \ . \tag{2.1.12}$$

It is noted that the off-diagonal elements are given from the next-leading operators.

We show an approximate form of the unitary matrix which diagonalizes the charged lepton mass matrix as $U_\ell M_\ell M_\ell^\dagger U_\ell^\dagger$:

$$U_\ell^\dagger \ \simeq \ \frac{1}{\sqrt{1+\alpha_\eta^{\tau^2}}} \begin{pmatrix} 1 & -\mathcal{O}(\alpha_\eta^2) & \alpha_\eta^\tau e^{i\varphi} \\ \mathcal{O}(\alpha_\eta^2) & \sqrt{1+\alpha_\eta^{\tau^2}} & \mathcal{O}(\alpha_\eta\lambda^4) \\ -\alpha_\eta^\tau e^{-i\varphi} & \mathcal{O}(\alpha_\eta^3) & 1 \end{pmatrix} \tag{2.1.13}$$

where

$$\alpha_\eta^\tau e^{i\varphi} \equiv \frac{y'_\tau}{y_\tau}\alpha_\eta. \tag{2.1.14}$$

The mass eigenvalues m_e^2, m_μ^2 and m_τ^2 are obtained in a good approximation as

$$m_e = |y_e|\alpha_\ell \lambda^4 v_d\ , \quad m_\mu = |y_\mu|\alpha_\ell \lambda^2 v_d\ , \quad m_\tau = |y_\tau|\alpha_\ell v_d\ , \tag{2.1.15}$$

where Yukawa coupling constants are $\mathcal{O}(1)$.

We find that the diagonalizing matrix U_ℓ depends on a real parameter α_η^τ and a phase factor φ in the leading order. We will show that the parameter α_η is much less than 1 in the numerical discussion, and the off-diagonal elements (1,3) and (3,1) in $U_\ell^\dagger$ have dominant contributions to the lepton mixing.

Neutrino mass matrix

It is useful to discuss an appropriated form of the neutrino mass matrix. The neutrino mass matrix is given from the superpotential w_ν in Eq. (2.1.3) and the VEV alignment in Eq.(2.1.10). The next-to-leading operators $llh_uh_u\phi_S\phi_T$ and $llh_uh_u\phi_T\xi$ can be suppressed and negligibly small since the factor $\langle\phi_T\rangle/\Lambda$ is small, which is confirmed in our numerical simulation. On the other hand, the operator $y_7' llh_uh_u\xi\eta$ cannot be neglected because $\langle\eta\rangle/\Lambda$ can be larger than $\langle\phi_T\rangle/\Lambda$. Then we have the following approximation by use of the multiplication rule of Appendix A:

$$\begin{aligned} w_\nu &\sim y_S v_u^2 \frac{v_S}{\Lambda^2}(\nu\nu)_{\mathbf{3}} \begin{pmatrix} 1\\1\\1\end{pmatrix}_{\mathbf{3}} + y_\xi v_u^2 (\nu\nu)_{\mathbf{1}} \frac{u}{\Lambda^2} + y_7' v_u^2 \alpha_\eta (\nu\nu)_{\mathbf{1'}} \frac{u}{\Lambda^2} \\ &= \frac{a}{3}\begin{pmatrix} 2\nu_1\nu_1 - \nu_2\nu_3 - \nu_3\nu_2 \\ 2\nu_3\nu_3 - \nu_1\nu_2 - \nu_2\nu_1 \\ 2\nu_2\nu_2 - \nu_3\nu_1 - \nu_1\nu_3 \end{pmatrix} \begin{pmatrix} 1\\1\\1\end{pmatrix} + c(\nu_1\nu_1 + \nu_2\nu_3 + \nu_3\nu_2) + d(\nu_3\nu_3 + \nu_1\nu_2 + \nu_2\nu_1) \end{aligned} \tag{2.1.16}$$

where y_S is redefined as $y_S \equiv y_S + y_5'\langle\eta\rangle/\Lambda$. The coefficients a, c and d are defined as:

$$a = \frac{y_S \alpha_\nu}{\Lambda} v_u^2\ , \quad c = \frac{y_\xi \alpha_\xi}{\Lambda} v_u^2\ , \quad d = \frac{y_7' \alpha_\xi \alpha_\eta}{\Lambda} v_u^2\ , \tag{2.1.17}$$

with

$$\alpha_\nu \equiv \frac{v_S}{\Lambda}\ , \qquad \alpha_\xi \equiv \frac{u}{\Lambda}\ . \tag{2.1.18}$$

The factor 1/3 of the first term is a convention. We can write the approximated neutrino mass matrix from Eq. (2.1.16) in a well-known form by introducing $b \equiv -a/3$:

$$M_\nu = a\begin{pmatrix} 1&0&0\\0&1&0\\0&0&1\end{pmatrix} + b\begin{pmatrix} 1&1&1\\1&1&1\\1&1&1\end{pmatrix} + c\begin{pmatrix} 1&0&0\\0&0&1\\0&1&0\end{pmatrix} + d\begin{pmatrix} 0&1&0\\1&0&0\\0&0&1\end{pmatrix}\ , \tag{2.1.19}$$

The magnitude of d is expected to be much smaller than a, b and c since the parameter d is induced from the next-to-leading operator $llh_uh_u\xi\eta$. We redefine a, c and d as follows:

$$a \to a\ , \quad c \to c\ e^{i\phi_c}\ , \quad d \to d\ e^{i\phi_d}\ , \tag{2.1.20}$$

where a, c and d are real; and the phase factors ϕ_c and ϕ_d can contribute to CP violation in the lepton flavor mixing. We have taken a to be real without loss of generality. We introduce a new basis of the neutrino mass matrix $\hat{M}_\nu$ defined with V_{TBM} as:

$$\hat{M}_\nu = V_{TBM}^T M_\nu V_{TBM} = \begin{pmatrix} a + ce^{i\phi_c} - \frac{d}{2}e^{i\phi_d} & 0 & -\frac{\sqrt{3}}{2}de^{i\phi_d} \\ 0 & ce^{i\phi_c} + de^{i\phi_d} & 0 \\ -p\frac{\sqrt{3}}{2}de^{i\phi_d} & 0 & a - ce^{i\phi_c} + \frac{d}{2}e^{i\phi_d} \end{pmatrix} . \quad (2.1.21)$$

It is noted that M_ν is diagonalized by TBM matrix for $d = 0$. We further consider a Hermitian matrix given by the neutrino mass matrix to discuss the neutrino mass eigenvalues and mixing:

$$\hat{M}_\nu \hat{M}_\nu^\dagger = \begin{pmatrix} (1,1) & 0 & (1,3) \\ 0 & |ce^{i\phi_c} + de^{i\phi_d}|^2 & 0 \\ (1,3)^* & 0 & (3,3) \end{pmatrix} , \quad (2.1.22)$$

where

$$\begin{aligned} (1,1) &= a^2 + c^2 + d^2 + 2ac\cos\phi_c - cd\cos(\phi_c - \phi_d) - ad\cos\phi_d \ , \\ (3,3) &= a^2 + c^2 + d^2 - 2ac\cos\phi_c - cd\cos(\phi_c - \phi_d) + ad\cos\phi_d \ , \\ (1,3) &= -\sqrt{3}\left[ad\cos\phi_d + icd\sin(\phi_c - \phi_d)\right] . \end{aligned} \quad (2.1.23)$$

The neutrino mixing matrix U_ν diagonalizes $\hat{M}_\nu \hat{M}_\nu^\dagger$ as

$$U_\nu \ (\hat{M}_\nu \hat{M}_\nu^\dagger) \ U_\nu^\dagger = \begin{pmatrix} m_1^2 & 0 & 0 \\ 0 & m_2^2 & 0 \\ 0 & 0 & m_3^2 \end{pmatrix} , \quad (2.1.24)$$

where the mass eigenvalues of neutrinos are written as follows:

$$\begin{aligned} m_1^2 &= a^2 + c^2 + d^2 - cd\cos(\phi_c - \phi_d) \\ &\quad - \sqrt{3c^2d^2\sin^2(\phi_c - \phi_d) + 4a^2(c^2\cos^2\phi_c + d^2\cos^2\phi_d - cd\cos\phi_c\cos\phi_d)} \ , \\ m_2^2 &= c^2 + d^2 + 2cd\cos(\phi_c - \phi_d) \ , \\ m_3^2 &= a^2 + c^2 + d^2 - cd\cos(\phi_c - \phi_d) \\ &\quad + \sqrt{3c^2d^2\sin^2(\phi_c - \phi_d) + 4a^2(c^2\cos^2\phi_c + d^2\cos^2\phi_d - cd\cos\phi_c\cos\phi_d)} \ , \end{aligned} \quad (2.1.25)$$

for NH ($m_1 < m_2 < m_3$). The neutrino mixing matrix U_ν is a 3×3 rotation matrix of 1-3 plane given as

$$U_\nu^\dagger = \begin{pmatrix} \cos\theta & 0 & \sin\theta e^{-i\sigma} \\ 0 & 1 & 0 \\ -\sin\theta e^{i\sigma} & 0 & \cos\theta \end{pmatrix} , \quad (2.1.26)$$

where θ and σ are written in terms of the model parameters as

$$\tan 2\theta = \sqrt{3}\,\frac{d\sqrt{a^2\cos^2\phi_d + c^2\sin^2(\phi_c - \phi_d)}}{a(d\cos\phi_d - 2c\cos\phi_c)} \ , \qquad \sigma = -\frac{c\sin(\phi_c - \phi_d)}{a\cos\phi_d} \ . \quad (2.1.27)$$

* * *

In the case of IH of neutrino masses, the neutrino mass eigenvalues cannot satisfy $\Delta m^2_{\rm sol} > 0$ for our calculation. The neutrino mass eigenvalues for IH case are given as

$$\begin{aligned} m_3^2 &= a^2 + c^2 + d^2 - cd\cos(\phi_c - \phi_d) \\ &\quad -\sqrt{3c^2d^2\sin^2(\phi_c-\phi_d) + 4a^2(c^2\cos^2\phi_c + d^2\cos^2\phi_d - cd\cos\phi_c\cos\phi_d)}\ , \\ m_1^2 &= a^2 + c^2 + d^2 - cd\cos(\phi_c - \phi_d) \\ &\quad +\sqrt{3c^2d^2\sin^2(\phi_c-\phi_d) + 4a^2(c^2\cos^2\phi_c + d^2\cos^2\phi_d - cd\cos\phi_c\cos\phi_d)}\ , \\ m_2^2 &= c^2 + d^2 + 2cd\cos(\phi_c - \phi_d)\ . \end{aligned} \tag{2.1.28}$$

One finds $\Delta m^2_{\rm sol} = m_2^2 - m_1^2$ as

$$\begin{aligned} \Delta m^2_{\rm sol} = c^2 \Bigg[& 3\frac{d}{c}\cos(\phi_c-\phi_d) - \frac{a^2}{c^2} \\ & - \sqrt{3\frac{d^2}{c^2}\sin^2(\phi_c-\phi_d) + 4\frac{a^2}{c^2}(\cos^2\phi_c + \frac{d^2}{c^2}\cos^2\phi_d - \frac{d}{c}\cos\phi_c\cos\phi_d)}\Bigg] \end{aligned} \tag{2.1.29}$$

It is impossible to obtain the observed value of $\Delta m^2_{\rm sol}$ since $a \sim c$ and $c \gg d$ in our model as seen in Eq.(2.1.17). Indeed, $d/c \propto \alpha_\eta$ is expected to be 0.07–0.3 in our numerical analysis.

2.1.5 PMNS matrix

We obtain the PMNS matrix as

$$U_{\rm PMNS} = U_\ell\ V_{\rm TBM}\ U_\nu^\dagger\ P\ , \tag{2.1.30}$$

where P is a diagonal matrix defined as

$$PU_\nu \hat{M}_\nu U_\nu^T P = {\rm diag}\{m_1, m_2, m_3\}, \tag{2.1.31}$$

so that m_1, m_2 and m_3 are real and positive neutrino masses. The three neutrino mixing angles can be written in terms of the model parameters in the leading order:

$$\begin{aligned} \sin\theta_{12} &\simeq \frac{1}{\sqrt{1+\alpha_\eta^{\tau 2}}}\frac{1}{\sqrt{3}}(1-\alpha_\eta^\tau e^{i\varphi})\ , \\ \sin\theta_{23} &\simeq -\frac{1}{\sqrt{2}}\cos\theta - \frac{1}{\sqrt{6}}\sin\theta e^{-i\sigma} \\ \sin\theta_{13} &\simeq \frac{1}{\sqrt{1+\alpha_\eta^{\tau 2}}}\left[\frac{2}{\sqrt{6}}\sin\theta e^{-i\sigma} - \frac{1}{\sqrt{2}}\alpha_\eta^\tau\cos\theta e^{i\varphi}\right]\ . \end{aligned} \tag{2.1.32}$$

2.2 Numerical discussion

We perform the numerical simulation of the model by use of the approximated results obtained from the previous section. We use the lepton mixing matrix appropriated as

$$U_\ell^\dagger \simeq \frac{1}{\sqrt{1+\alpha_\eta^{\tau 2}}}\begin{pmatrix} 1 & 0 & \alpha_\eta^\tau e^{i\varphi} \\ 0 & \sqrt{1+\alpha_\eta^{\tau 2}} & 0 \\ -\alpha_\eta^\tau e^{-i\varphi} & 0 & 1 \end{pmatrix}, \tag{2.2.1}$$

and the neutrino mass matrix of Eq. (2.1.19), which enables us to discuss correlations among the model parameters and numerical results. The tau lepton mass determines α_ℓ. The real parameters a and c are fixed by the observed value of $\Delta m^2_{\rm sol}$ and $\Delta m^2_{\rm atom}$. We note that the magnitude of d is related to α_η as

$$\alpha_\eta^\nu \equiv \frac{d}{c} = \left|\frac{y_7'}{y_\xi}\right| \alpha_\eta \tag{2.2.2}$$

Thus, we have the following model parameters:

$$m_1, \quad \alpha_\eta, \quad \varphi, \quad \phi_c, \quad \phi_d, \tag{2.2.3}$$

under the assumption: $\alpha_\eta = \alpha_\eta^\tau = \alpha_\eta^\nu$ i.e. $|y_7'/y_\xi| = |y_\tau'/y_\tau| = 1$, which is reasonable since the Yukawa couplings are taken to be order one. The lightest neutrino mass eigenvalue m_1 is limited by the cosmological observation $\sum m_i < 160$ [meV] [98–100]. We scan the phase factors φ, ϕ_c and ϕ_d in $[-\pi, \pi]$. We explain how to scan α_η in the next subsection.

2.2.1 Gamma distribution

Our numerical discussion is robust if

$$\lambda \ll 1, \quad \alpha_\ell \ll 1, \quad \alpha_\eta \ll 1. \tag{2.2.4}$$

The small λ is obtained from the charged lepton mass hierarchy as seen Eq. (2.1.15) for the Yukawa couplings of order one. The value of α_ℓ is fixed by m_τ from Eq. (2.1.15), which leads to

$$\alpha_\ell = 0.0316\,(0.010), \tag{2.2.5}$$

where we assume two cases: $\tan\beta = v_u/v_d = 3\,(0)$ ($\sqrt{v_u^2+v_d^2} = v/\sqrt{2}$ where $v = 246$ [GeV]) in $|y_\tau| = 1$ unit. The VEV alignment Eq.(2.1.10) leads to the following relation:

$$\alpha_\eta = \frac{\lambda_1}{\lambda_2}\sqrt{\frac{g_4}{3g_3}}\,\alpha_\ell\ . \tag{2.2.6}$$

In order to remove $\alpha_\eta > 0.3$ for a good approximation, we scan the coefficient before α_ℓ in Eq.(2.2.6) in the following method.

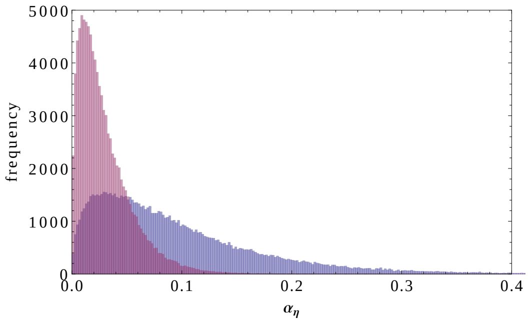

Figure 2.2.1: The distribution of α_η for $\alpha_\ell = 0.0316$ (blue) and $\alpha_\ell = 0.010$ (red) in Eq.(2.2.8) ($\alpha = 3/2, \beta = 2, \gamma = 1, \mu = 0$). This figure is taken from [27].

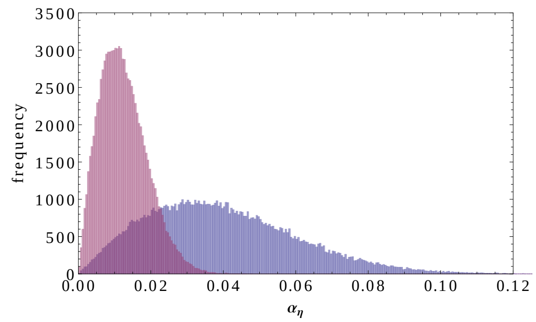

Figure 2.2.2: The distribution of α_η for $\alpha_\ell = 0.0316$ (blue) and $\alpha_\ell = 0.010$ (red) in Eq.(2.2.9) ($\alpha = 1, \beta = \sqrt{2}, \gamma = 2, \mu = 0$). This figure is taken from [27].

The value of α_η is given by the Gamma distribution which is useful to distribute order one parameters:

$$f = (x-\mu)^{(\alpha\gamma-1)} e^{\left(-\frac{x-\mu}{\beta}\right)^\gamma} . \tag{2.2.7}$$

When we take $\gamma = 1$ with $\alpha = 3/2$, $\mu = 0$ and $\beta = 2$, we have

$$f = \sqrt{x}\; e^{-\frac{1}{2}x} , \tag{2.2.8}$$

which is identical to the χ^2 distribution. We also consider alternative distribution given by $\gamma = 2$ with $\alpha = 1$, $\mu = 0$ and $\beta = \sqrt{2}$:

$$f = x\; e^{-\frac{1}{2}x^2} , \tag{2.2.9}$$

which behaves like the Gaussian distribution.

We obtain $\alpha_\eta = f\alpha_\ell$. We show the distribution of α_η in Figs. 2.2.1 and 2.2.2 for $\alpha_\ell = 0.0316$ and $\alpha_\ell = 0.010$ based on the two cases Eqs.(2.2.8) and (2.2.9).

In advance, we comment on the results from different distributions of α_η presented in Eq. (2.2.8) and (2.2.9). We have found that our results from the two Gamma distributions do not make a significant change for both the different values $\alpha_\ell = 0.0316$ nor 0.010. Moreover, we have scanned α_η in the flat-distribution for $0 \leq \alpha_\eta \leq 0.3$ and the results do not change. Therefore, we use Eq. (2.2.8) for $\alpha_\ell = 0.0316$ in the following discussion.

2.2.2 Results

We present the prediction for the mixing angles θ_{12}, θ_{23} and the CP violating phases δ_{CP}, α_{21}, α_{31} as well as the effective mass for the $0\nu\beta\beta$ decay $\langle m_{ee}\rangle$. We have used the global fit given from NuFIT 3.2 [3] shown in in Tab. 2.2.1. We show the results which satisfy the observation in 1σ C.L. by green points and 3σ C.L. by blue points.

The predicted δ_{CP} and $\sin^2\theta_{23}$ are shown in Fig. 2.2.2. The red curve represents TM_2 prediction which is obtained when we turn off the charged lepton mixing artificially. It

observable	best fit and $1\,\sigma$	$3\,\sigma$ range
$\Delta m^2_{\rm atm}$	$(2.494^{+0.033}_{-0.031}) \times 10^{-3}{\rm eV}^2$	$(2.399 \sim 2.593) \times 10^{-3}{\rm eV}^2$
$\Delta m^2_{\rm sol}$	$(7.40^{+0.21}_{-0.20}) \times 10^{-5}{\rm eV}^2$	$(6.80 \sim 8.02) \times 10^{-5}{\rm eV}^2$
$\sin^2\theta_{23}$	$0.538^{+0.033}_{-0.069}$	$0.418 \sim 0.613$
$\sin^2\theta_{12}$	$0.307^{+0.013}_{-0.012}$	$0.272 \sim 0.346$
$\sin^2\theta_{13}$	$0.02206^{+0.00075}_{-0.00075}$	$0.01981 \sim 0.02436$

Table 2.2.1: The neutrino oscillation parameters from NuFIT 3.2 for NH [3].

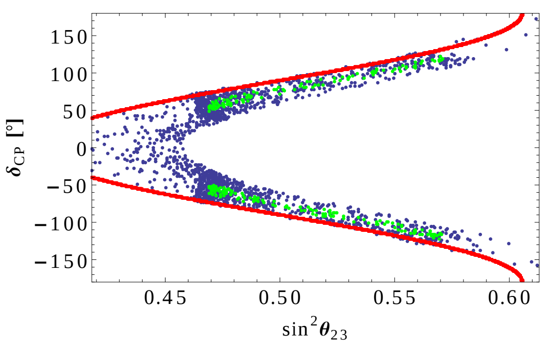

Figure 2.2.3: The predicted $\sin\theta_{23}$ and δ_{CP}. The red curve denotes the prediction from TM_2. This figure is taken from [27]

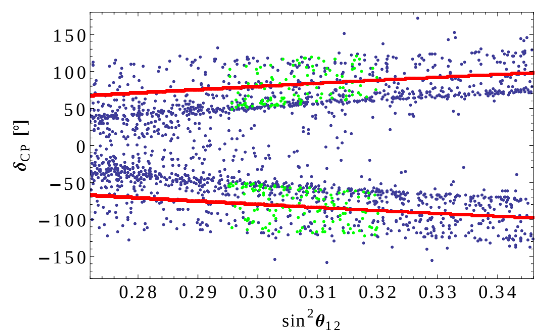

Figure 2.2.4: The predicted $\sin\theta_{12}$ and δ_{CP}. The red curve are given by TBM neutrino mixing. This figure is taken from [27].

may be helpful to see the effect from the charged lepton sector. The Dirac CP violating phase δ_{CP} is allowed in $[-\pi, \pi]$ for 3σ C.L.. One finds a typical prediction of TM_2: δ_{CP} is expected to be $|60°\text{–}90°|$ for $\theta_{23} = \pi/4$. At the best fit $\sin^2\theta_{23} = 0.538$, we find $90° \lesssim |\delta_{CP}| \lesssim 110°$. One also finds $|\delta_{CP}|$ is predicted to be $50°\text{–}120°$ with the constraint of 1σ C.L. data ,which may be favored for the current observation.

We also show the prediction of δ_{CP} and $\sin^2\theta_{12}$ in Fig. 2.2.2. The red curve denotes only TBM neutrino mixing with the charged lepton mixing, which is obtained by $d = 0$ and best best fit data in Tab. 2.2.1. It may be useful to see the effect of 1-3 rotation in the neutrino mixing. One can find that $|\delta_{CP}|$ is predicted as $[60°, 120°]$ at the best fit of $\sin^2\theta_{12} = 0.307$, which may be also favored in the future observation.

The prediction of the Majorana phases α_{21} and α_{31} is shown in Fig. 2.2.2. One finds a clear correlation between both phases. Both α_{21} and α_{31} are allowed in $[-\pi, \pi]$.

In Fig. 2.2.2, we show the predicted $|m_{ee}|$ in terms of the lightest neutrino mass eigenvalue m_1. the predicted $|m_{ee}|$ is $[10, 45]\,\mathrm{meV}$. The lightest neutrino mass m_1 is predicted for $m_1 > 12\,\mathrm{meV}$, which is required by the observed mass squared differences. The upper bound $m_1 < 46\,\mathrm{meV}$ is derived from the cosmological constraint [98].

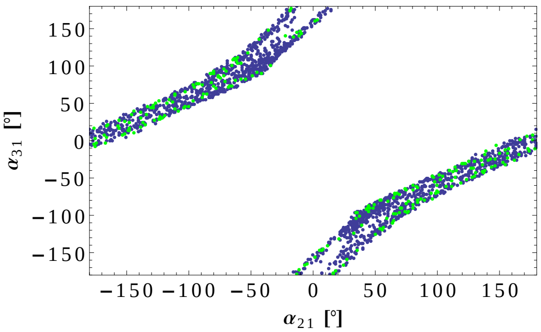

Figure 2.2.5: The allowed regions of the Majorana phases. This figure is taken from [27].

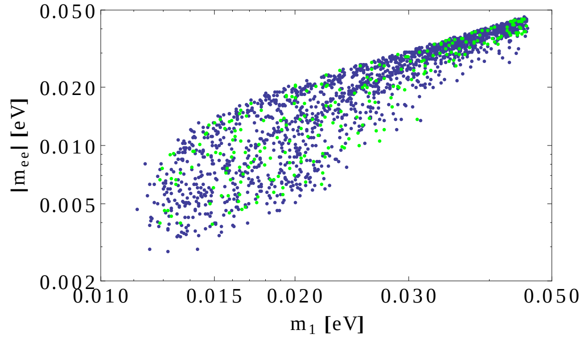

Figure 2.2.6: The prediction of $\langle m_{ee} \rangle$ and the lightest neutrino mass m_1. This figure is taken from [27].

2.3 Chapter summary

The flavor symmetry is a powerful approach to study the flavor mixing theoretically. The Yukawa couplings can take order one values. The VEVs of the additional scalar fields realizes not only the charged lepton mass hierarchy but also the observed lepton mixing angles.

We have reviewed a model of flavor symmetry with A_4 and Z_3 [27]. The model requires several flavons in order to obtain the consistent mass hierarchy of the charged leptons and the neutrino mixing parameters. A potential analysis of the flavons is also available. The light neutrino mass is induced by the Weinberg operator. It is remarkable that the flavon η couples to the charged lepton sector as well as the neutrino sector, and it provides us a widely acceptable predictions for the lepton mixing angles. In our approximated discussions, we have found many relations among the observable and the model parameters. We have also performed numerical studies within a good approximation; and found that the predicted Dirac CP violating phase and the mixing angle θ_{23} are expected to be favored for the future observations of the neutrino oscillation experiments. It is also remarkable that the model can predict the Majorana phases and $\langle m_{ee} \rangle$ which can be detected if the neutrinos are Majorana particles. It may be a test for the model in the future.

We have confirmed that an approach by use of flavor symmetry can afford to predict the three mixing angle and the Dirac CP violating phase which are consistent to the global fit in 1σ C.L.. In the next chapter, we show an alternative method which does not assume a specific flavor symmetry.

Chapter 3

Texture zeros

We show another approach to the lepton flavor mixing. We discuss the flavor structure based on the experimental results without flavor symmetry, which is often called as a top-down approach. We have seen that we construct the charged lepton mass matrix and neutrino mass matrix from a flavor symmetric theory, a bottom-up approach. It is also important to determine what kind of texture of the mass matrix is available in order to make a minimal model of flavor symmetry. In other words, it will be a guide for the minimal theory of flavor symmetry. We will show the two textures so as to induce the following PMNS matrices:

$$\begin{aligned}
\mathrm{TM}_1 &: U_{PMNS} = V_{TBM} O_{23}, \\
\mathrm{TM}_2 &: U_{PMNS} = V_{TBM} O_{13}.
\end{aligned}$$

The rotation matrix of i-j plane O_{ij} gives rise to a deviation from the TBM mixing, which is expected to be realized by non-Abelian discrete group. The model in the previous chapter gives approximately TM_2. We note that TM_3 is not available since it predicts $\theta_{13} = 0$.

3.1 Minimal texture

We introduce only two right-handed Majorana neutrinos N_1 and N_2, which is possible though the lightest neutrino mass vanishes $m_1 = 0$ for NH ($m_3 = 0$ for IH). Then, we have 3×2 the Dirac neutrino mass matrix and 2×2 right-handed Majorana neutrino mass matrix. We also set the charged lepton mass matrix to be diagonal without loss of generality.

Let us study the type I seesaw model of the minimal texture. We can take a diagonal basis of the 2×2 right-handed Majorana neutrino mass matrix M_R:

$$M_R = \begin{pmatrix} M_1 & 0 \\ 0 & M_2 \end{pmatrix} = M_0 \begin{pmatrix} p^{-1} & 0 \\ 0 & 1 \end{pmatrix}, \tag{3.1.1}$$

where we define M_0 and $p = M_2/M_1$. The generic form of 3×2 Dirac neutrino mass matrix M_D can be paramterize

$$M_D = vY_\nu = v \begin{pmatrix} a & d \\ b & e \\ c & f \end{pmatrix}, \tag{3.1.2}$$

where $v = 174.1$ GeV and the elements a, b, c, d, e, f are complex. The effective left-handed Majorana neutrino mass matrix M_ν is obtained by the type I seesaw mechanism:

$$M_\nu = -M_D M_R^{-1} M_D^T = -\frac{v^2}{M_0} \begin{pmatrix} a^2p + d^2 & abp + de & acp + df \\ abp + de & b^2p + e^2 & bcp + ef \\ acp + df & bcp + ef & c^2p + f^2 \end{pmatrix}. \tag{3.1.3}$$

It is useful to discuss the TBM mixing basis of the neutrino mass matrix:

$$\hat{M}_\nu \equiv V_{\text{TBM}}^T M_\nu V_{\text{TBM}} = -\frac{v^2}{M_0} \begin{pmatrix} \frac{A_\nu^2 p + D_\nu^2}{6} & \frac{A_\nu B_\nu p + D_\nu E_\nu}{3\sqrt{2}} & \frac{A_\nu C_\nu p + D_\nu F_\nu}{2\sqrt{3}} \\ \frac{A_\nu B_\nu p + D_\nu E_\nu}{3\sqrt{2}} & \frac{B_\nu^2 p + E_\nu^2}{3} & \frac{B_\nu C_\nu p + E_\nu F_\nu}{\sqrt{6}} \\ \frac{A_\nu C_\nu p + D_\nu F_\nu}{2\sqrt{3}} & \frac{B_\nu C_\nu p + E_\nu F_\nu}{\sqrt{6}} & \frac{C_\nu^2 p + F_\nu^2}{2} \end{pmatrix}, \tag{3.1.4}$$

where

$$\begin{aligned} A_\nu &\equiv 2a - b - c, \qquad & B_\nu &\equiv a + b + c, \qquad & C_\nu &\equiv c - b, \\ D_\nu &\equiv 2d - e - f, \qquad & E_\nu &\equiv d + e + f, \qquad & F_\nu &\equiv f - e. \end{aligned} \tag{3.1.5}$$

We find the minimal texture by imposing zero in the Dirac mass matrix elements and comparing its predictions and the observations. TM_1 and TM_2 are expected to be consistent and minimal. In this thesis, we discuss only for TM_1 for the case with NH of neutrino masses.

We present the neutrino mass matrix for TM_1 in NH case. One can find that it is realized if $\hat{M}_\nu$ satisfies

$$A_\nu = 0 \quad \text{and} \quad D_\nu = 0. \tag{3.1.6}$$

Then we have

$$\hat{M}_\nu = -\frac{v^2}{M_0} \begin{pmatrix} 0 & 0 & 0 \\ 0 & \frac{3}{4}\left((b+c)^2 p + (e+f)^2\right) & \frac{1}{2}\sqrt{\frac{3}{2}}\left((c^2 - b^2)p - e^2 + f^2\right) \\ 0 & \frac{1}{2}\sqrt{\frac{3}{2}}\left((c^2 - b^2)p - e^2 + f^2\right) & \frac{1}{2}\left((b-c)^2 p + (e-f)^2\right) \end{pmatrix}, \tag{3.1.7}$$

where $p = M_1/M_2$. The efective neutrino mass matrix derives from the following Dirac neutrino mass matrix:

$$M_D = vY_\nu = v \begin{pmatrix} \frac{b+c}{2} & \frac{e+f}{2} \\ b & e \\ c & f \end{pmatrix}. \tag{3.1.8}$$

It is noted that a redefinitions of the left-handed lepton fields allows to take e and f to be real. We set only b and c to be complex without loss of generality. The minimal texture is obtained by an additional condition on Eq. (3.1.8). There are three as follows [42]:

$$\text{(I) } b+c=0, \qquad \text{(II) } c=0, \qquad \text{(III) } b=0. \tag{3.1.9}$$

These conditions lead to the following Dirac neutrino mass matrices:

$$M_D = \begin{cases} v\begin{pmatrix} 0 & \frac{e+f}{2} \\ b & e \\ -b & f \end{pmatrix} & \text{for (I)} \\ v\begin{pmatrix} \frac{b}{2} & \frac{e+f}{2} \\ b & e \\ 0 & f \end{pmatrix} & \text{for (II)} \\ v\begin{pmatrix} \frac{c}{2} & \frac{e+f}{2} \\ 0 & e \\ c & f \end{pmatrix} & \text{for (III)} \end{cases} . \tag{3.1.10}$$

We obtain the effective neutrino mass matrix in the TBM basis $\hat{M}_\nu$ for I case as:

$$\hat{M}_\nu^{\mathrm{I}} = -\frac{f^2v^2}{M_0}\begin{pmatrix} 0 & 0 & 0 \\ 0 & \frac{3}{4}(k+1)^2 & -\frac{1}{2}\sqrt{\frac{3}{2}}(k^2-1) \\ 0 & -\frac{1}{2}\sqrt{\frac{3}{2}}(k^2-1) & 2B^2pe^{2i\phi_B}+\frac{1}{2}(k-1)^2 \end{pmatrix}, \tag{3.1.11}$$

where we redefine the new real parameters k, B and ϕ_B as

$$k \equiv \frac{e}{f}, \qquad \phi_B \equiv \arg[b], \qquad B \equiv \frac{|b|}{f}. \tag{3.1.12}$$

We also obtain $\hat{M}_\nu$ for II as

$$\hat{M}_\nu^{\mathrm{II}} = -\frac{f^2v^2}{M_0}\begin{pmatrix} 0 & 0 & 0 \\ 0 & \frac{3}{4}[\hat{B}^2pe^{2i\phi_B}+(k+1)^2] & -\frac{1}{2}\sqrt{\frac{3}{2}}[\hat{B}^2pe^{2i\phi_B}+k^2-1] \\ 0 & -\frac{1}{2}\sqrt{\frac{3}{2}}[\hat{B}^2pe^{2i\phi_B}+k^2-1] & \frac{1}{2}[\hat{B}^2pe^{2i\phi_B}+(k-1)^2] \end{pmatrix}, \tag{3.1.13}$$

where the real parameters are defined as

$$k \equiv \frac{e}{f}, \qquad \phi_B \equiv \arg[b], \qquad \hat{B} \equiv \frac{|b|}{f}. \tag{3.1.14}$$

We also obtain $\hat{M}_\nu$ for III as

$$\hat{M}_\nu^{\mathrm{III}} = -\frac{f^2v^2}{M_0}\begin{pmatrix} 0 & 0 & 0 \\ 0 & \frac{3}{4}[B^2pe^{2i\phi_B}+(k+1)^2] & -\frac{1}{2}\sqrt{\frac{3}{2}}[-B^2pe^{2i\phi_B}+k^2-1] \\ 0 & -\frac{1}{2}\sqrt{\frac{3}{2}}[-B^2pe^{2i\phi_B}+k^2-1] & \frac{1}{2}[B^2pe^{2i\phi_B}+(k-1)^2] \end{pmatrix}. \tag{3.1.15}$$

It is noted that real parameters are defined differently from case I as

$$k \equiv \frac{e}{f}, \qquad \phi_B \equiv \arg[c], \qquad B \equiv \frac{|c|}{f}\ . \tag{3.1.16}$$

The formulations and numerical simulations for the minimal textures TM_1 as well as TM_2 are presented for both NH and IH cases in Ref. [47]:

3.2 Neutrino mass and mixing matrix

We represent the neutrino mass eigenvalues and neutrino mixing parameters including the CP violating phase in terms of the model parameters. Note that the definition of k, B and ϕ_B differs in each case.

The neutrino masses are given follows:

$$\begin{aligned} m_1 = 0, \qquad & m_2^2 m_3^2 = \frac{9v^8}{4M_0^4}(j-k)^4 f^8 B^4 p^2, \\ m_2^2 + m_3^2 = & \frac{v^4 f^4}{16M_0^2}\left[B^4p^2(5j^2+2j+5)^2\right. \\ & \left. +2B^2p(5jk+j+k+5)^2\cos 2\phi_B + (5k^2+2k+5)^2\right] \end{aligned} , \tag{3.2.1}$$

where we have introduced $j \equiv b/c$. The cases I, II and III correspond $j=-1$, $j=\infty$ and $j=0$ respectively. For case II, we further set $B = c/f \to 0$ and $\hat{B} = Bj$ is finite. We fix the model parameters $B\sqrt{p}$ and f^2/M_0 by two mass squared differences, and the other mixing parameters and observables are predicted from two parameters: k and ϕ_B.

The PMNS matrix is obtained by a 2-3 plane rotation matrix O_{23} for TM_1 texture. We parametrize O_{23} as

$$O_{23} = \frac{1}{\mathcal{A}}\begin{pmatrix} \mathcal{A} & 0 & 0 \\ 0 & 1 & \mathcal{V} \\ 0 & -\mathcal{V}^* & 1 \end{pmatrix}, \qquad \mathcal{A} = \sqrt{1+|\mathcal{V}|^2}\ , \tag{3.2.2}$$

For case I:

$$\mathcal{V} = -\frac{f^2v^4}{M_0^2}\frac{\sqrt{6}(k^2-1)[(5k^2+2k+5)+8B^2p\ e^{2i\phi_B}]}{16m_3^2 + 3\frac{f^4v^4}{M_0^2}(k+1)^2(5k^2+2k+5)}\ . \tag{3.2.3}$$

For case II:

$$\mathcal{V} = -\frac{f^2v^4}{M_0^2}\frac{\sqrt{6}\,[(k^2-1)(5k^2+2k+5)+5B^4p^2+2B^2p(5k+1)(k\cos 2\phi_B + i\sin 2\phi_B)]}{16m_3^2 - 3\frac{f^4v^4}{M_0^2}\,[(k+1)^2(5k^2+2k+5)+5B^4p^2+2B^2p(k+1)(5k+1)\cos 2\phi_B]}. \tag{3.2.4}$$

For case Ⅲ:

$$\mathcal{V} = -\frac{f^2v^4}{M_0^2}\frac{\sqrt{6}\,[(k^2-1)(5k^2+2k+5)-5B^4p^2-2B^2p(k+5)(\cos 2\phi_B+ik\sin 2\phi_B)]}{16m_3^2-3\frac{f^4v^4}{M_0^2}\,[(k+1)^2(5k^2+2k+5)+5B^4p^2+2B^2p(k+1)(k+5)\cos 2\phi_B]}. \tag{3.2.5}$$

The CP violating measure J_{CP} [92] is written in terms of $\mathcal{V}$ as

$$J_{CP} \equiv \mathrm{Im}\left[U_{e1}U_{\mu 2}U_{e2}^*U_{\mu 1}^*\right] = -\frac{1}{3\sqrt{6}\mathcal{A}^2}\mathrm{Im}[\mathcal{V}^*]\ , \tag{3.2.6}$$

3.3 Dirac CP violating phase

The only source of the CP violation is ϕ_B for these minimal texture models. It will be interesting to discuss the Dirac CP violating phase in detail. The Jarlskog invariant J_{CP} can be related to the mass matrices of the charged leptons M_ℓ and neutrinos M_ν. We have used a basis where the charged lepton mass matrix is diagonal: $M_\ell = \mathrm{diag}[m_e, m_\mu, m_\tau]$. We use another CP violating measure $\mathcal{J}_{CP}$ [101, 102]:

$$\mathcal{J}_{CP} = \mathrm{Tr}\left[(M_\nu M_\nu^\dagger)^*, (M_\ell M_\ell^\dagger)\right]^3 = -6i\Delta m_\ell^6 \Delta m_\nu^6 J_{CP}\ , \tag{3.3.1}$$

where Δm_ℓ^6 and Δm_ν^6 are mass parameters given as

$$\begin{aligned}\Delta m_\ell^6 &\equiv (m_\mu^2 - m_e^2)(m_\tau^2 - m_\mu^2)(m_\tau^2 - m_e^2),\\ \Delta m_\nu^6 &\equiv (m_2^2 - m_1^2)(m_3^2 - m_2^2)(m_3^2 - m_1^2),\end{aligned} \tag{3.3.2}$$

respectively. We can rewrite Δm_ν^6 as

$$\begin{aligned}\Delta m_\nu^6 &= (m_2^2 - m_1^2)(m_3^2 - m_2^2)(m_3^2 - m_1^2)\\ &= \Delta m_{21}^2(\Delta m_{31}^2 - \Delta m_{21}^2)\Delta m_{31}^2,\end{aligned} \tag{3.3.3}$$

where $\Delta m_{ij}^2 \equiv m_i^2 - m_j^2$. Since the neutrino oscillation experiments have revealed that Δm_{31}^2 is much larger than Δm_{21}^2 for NH, the neutrino mass parameter Δm_ν^6 is always positive for NH.

We can calculate $\mathcal{J}_{CP}$ for each case and find

$$\text{case I}: \quad J_{CP} = -\frac{3}{8}\frac{f^{12}}{M_0^6}(B\sqrt{p})^6(k-1)(k+1)^5\sin 2\phi_B\frac{v^{12}}{\Delta m_\nu^6}\ , \tag{3.3.4}$$

$$\text{case II}: \quad J_{CP} = -\frac{3}{32}\frac{f^{12}}{M_0^6}(B\sqrt{p})^6(5k+1)\sin 2\phi_B\frac{v^{12}}{\Delta m_\nu^6}\ , \tag{3.3.5}$$

$$\text{case III}: \quad J_{CP} = \frac{3}{32}\frac{f^{12}}{M_0^6}(B\sqrt{p})^6k^5(k+5)\sin 2\phi_B\frac{v^{12}}{\Delta m_\nu^6}\ . \tag{3.3.6}$$

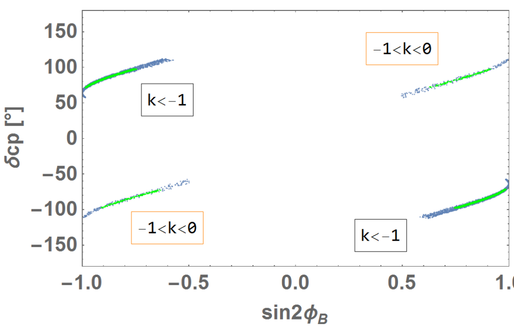

Figure 3.3.1: The prediction of ϕ_B with δ_{CP}. The blue and green dots are consistent to the given results at 3σ and 1σ C.L. respectively. This figure is taken from [47].

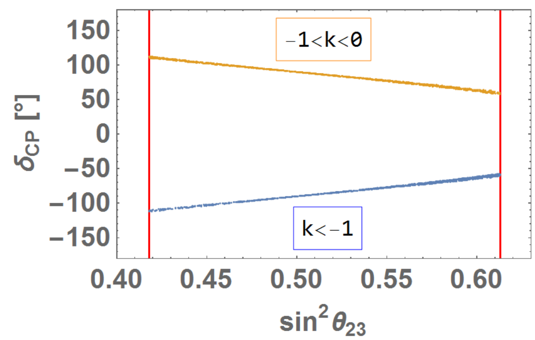

Figure 3.3.2: The predicted $\sin^2\theta_{23}$ and δ_{CP} for $\sin 2\phi_B > 0$. The blue and orange dots represent the predictions for $k < -1$ and $-1 < k < 0$ respectively. This figure is taken from [104].

We obtain clear a relation between the sign of J_{CP} and k for each case:

$$J_{CP} \propto \begin{cases} \sin 2\phi_B \text{ for } -1 \le k \le 1 & ; -\sin 2\phi_B \text{ for } k \le -1, k \ge 1 \quad : \text{case I} \\ \sin 2\phi_B \text{ for } k \le -1/5 & ; -\sin 2\phi_B \text{ for } k \ge -1/5 \quad : \text{case II} \\ \sin 2\phi_B \text{ for } k \le -5, k \ge 0 & ; -\sin 2\phi_B \text{ for } -5 \le k \ge 0 \quad : \text{case III} \end{cases} \tag{3.3.7}$$

It is noted that the sign of $\sin 2\phi_B$ must be positive in order to obtain the observed baryon–entropy ratio η_B [103]

$$\eta_B \equiv \frac{n_B}{s} = [5.8, 6.6] \times 10^{-10}, \tag{3.3.8}$$

as discussed in Ref. [104], where $n_B = n_b - n_{\bar{b}}$ is the baryon number density and s is the entropy density. In Ref. [104], we confirmed that TM_1 for IH case and TM_2 for both NH and IH cases have no contribution to the baryon asymmetry.

We show predictions of the Dirac CP violating phase from the above minimal texture. We scan k in a range $[-20, 20]$ and ϕ_B in $[-\pi, \pi]$ for our numerical simulation. The minimal texture gives us clear predictions and correlations. In Fig. 3.3.1, one finds a clear correlation between δ_{CP} and $\sin 2\phi_B$. The blue and green dots satisfy the experimental bounds with 3σ and 1σ C.L. respectively. The predicted magnitude $|\delta_{CP}|$ is allowed in $[110°, 115°]$ for 1σ C.L. and $[45°, 125°]$ for 3σ C.L.. The four separated regions are distinguished by the value of k. It is remarkable that we can predict δ_{CP} up to its sign. The sign of δ_{CP} is determined in accordance with Eq. (3.3.7).

We also show the predicted $\sin^2\theta_{23}$ in terms of δ_{CP} in Fig. 3.3.2. The red lines denotes upper and lower bound obtained from the data of 3σ C.L.. The prediction is limited for $\sin 2\phi_B > 0$ as mentioned above. Blue and orange dots represent the prediction for $k < -1$ and $-1 < k < 0$ respectively. It is noted that the maximal mixing $\theta_{23} = \pi/4$ and CP violation $\delta_{CP} = \pm 90°$ can be realized.

One can finds other discussions and figures in Refs. [47, 104]

3.4 Chapter summary

We have discussed a top-down approach which does not specify a flavor symmetry. It is useful to discuss the minimal texture consistent to the experimental results in a phenomenological point of view. A model with a large number of model parameters cannot provide a testable prediction. To discuss both top-down approach and bottom-up approach will lead to a minimal theory of flavor. Our model has 3×2 Dirac neutrino mass matrix, which is realized S_4 flavor symmetry. To consider a specific VEV alignment which gives our minimal texture will be interesting.

We have reviewed a texture zeros approach where two right-handed neutrinos are introduced [47]. The light neutrino mass is obtained by the type I seesaw mechanism. We have discussed only for NH case in TM_1 texture. The number of model parameters is only four: $k, \phi_B, B\sqrt{p}$ and f^2/M_0. It is remarked that the mixing parameters, effective mass $\langle m_{ee} \rangle$ and Majorana CP violating phases are determined only by k and ϕ_B after we fix $B\sqrt{p}$ and f^2/M_0 by the neutrino mass squared differences.

The most important result is the predicted Dirac CP violating phase. The minimal texture enables us to distinguish the sign of δ_{CP} by specific sets of k and ϕ_B. Moreover, the cosmological observation of BAU requires $\sin \phi_B > 0$ as discussed in Ref [104]. In other words, the key parameter k determines the sign of Dirac CP violating phase.

In the next chapter, we discuss a new approach for flavor symmetry which does not require a additional gauge singlet scalar field such as flavon. It also can be a minimal model because of the small number of parameters.

Chapter 4

Modular invariant theory

We consider a six-dimensional compact space X_6 in superstring theory. Suppose that the six-dimensional compact space has a two-dimensional compact space X_2. The lepton mixing can be determined by a flavor symmetry originated from the modular symmetry defined in X_2. The other extra four-dimensional space contributes to an overall factor of Yukawa couplings. We discuss a modular invariant model that is symmetric under the A_4 transformations in a supersymmetric model [52]

4.1 Flavor symmetry from modular group

The recent achievement in the flavor symmetry supposes the theory has modular invariance and the non-Abelian discrete groups such as S_3, A_4, S_4, A_5 are obtained as quotient groups of the modular group. The Yukawa couplings are written as modular modular forms and transform non-trivially under the modular transformation. We briefly review a method of the modular invariant flavor theory [50].

4.1.1 Modular group

The modular group Γ is generated by the following transformation for a complex parameter called the modulus τ:

$$\tau \longrightarrow \frac{a\tau + b}{c\tau + d}, \quad \{a, b, c, d \in \mathbb{Z} : ad - bc = 0, \quad \mathrm{Im}[\tau] > 0\}, \tag{4.1.1}$$

This is called the modular transformation. We can understand it geometrically by considering a change of the two basis vectors into another basis generated from two different lattice points in a 2-dimensional complex plane of Fig. 4.1.1:

$$\begin{pmatrix} \alpha_2' \\ \alpha_1' \end{pmatrix} = \gamma \begin{pmatrix} \alpha_2 \\ \alpha_1 \end{pmatrix}, \quad \gamma = \begin{pmatrix} a & b \\ c & d \end{pmatrix}, \quad \tau \equiv \frac{\alpha_2}{\alpha_1}. \tag{4.1.2}$$

The infinite modular group Γ is generated by the two generators, $\gamma = S$ and T:

$$S = \begin{pmatrix} 0 & 1 \\ -1 & 0 \end{pmatrix}, \quad T = \begin{pmatrix} 1 & 1 \\ 0 & 1 \end{pmatrix}. \tag{4.1.3}$$

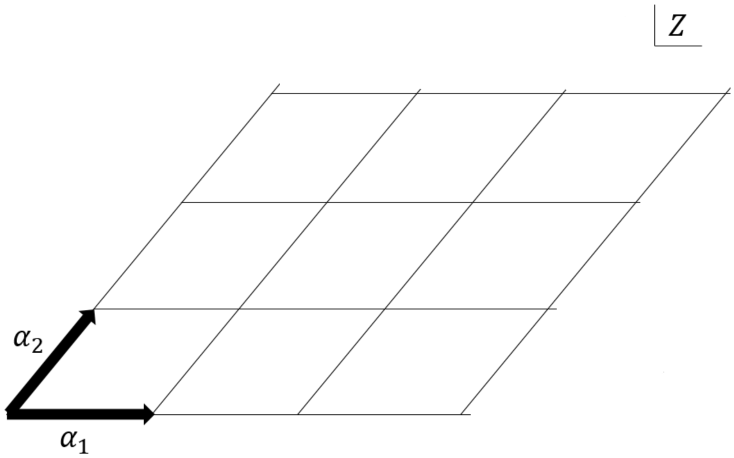

Figure 4.1.1: A lattice spaned by basis vectors $\alpha_1 = 2\pi R$ and $\alpha_2 = 2\pi R\tau$ in a 2D complex plane. These are parametrized by $R \in \mathbb{R}$ and $\tau \in \mathbb{C}$.

It is equivalent with

$$S : \tau \to -\frac{1}{\tau}, \quad T : \tau \to \tau + 1. \tag{4.1.4}$$

We can obtain the quotient subgroup $\Gamma_N = \Gamma/\Gamma(N)$ isomorphic to S_3, A_4, S_4 and A_5 with $N = 2, 3, 4$ and 5 respectively, where $\Gamma(N)$ is a finite subgroup of Γ obtained by the congruence condition:

$$T^N = 1. \tag{4.1.5}$$

It is noted that T transformation matrix of Eq.(4.1.5) is no longer the T of Eq.(4.1.3).

4.1.2 Modular invariance

The new type of flavor symmetry model is invariant under Γ_N in addition to the continuous gauge groups of SM. We have a natural derivation of the modular transformation for the chiral superfields in $N = 1$ global supersymmetry. It will be provided in an extension to the $N = 1$ supergravity theory from supersymmetry.

Let us consider the modular invariance of the $N = 1$ supergravity Lagrangian

$$G(\tau, \bar{\tau}) = m_p^{-2} K(\tau, \bar{\tau}) + \ln W(\tau) + \ln \bar{W}(\bar{\tau}), \tag{4.1.6}$$

where $K(\tau, \bar{\tau})$ and $W(\tau)$ denotes the Kähler potential and superpotential respectively. The Kähler potential is a real function and the coefficient m_p is the reduced Planck mass scale:

$$m_p \equiv \frac{M_p}{\sqrt{8\pi}} = \sqrt{\frac{\hbar c}{8\pi G}}. \tag{4.1.7}$$

The supergravity Lagrangian G is required to be invariant under the transformation of Γ_N. The modular invariance of G is realized by the Kähler invariance:

$$\begin{cases} K(\tau,\bar{\tau}) \longrightarrow K(\tau,\bar{\tau}) + F(\tau) + \bar{F}(\bar{\tau}) \\ W(\tau) \longrightarrow e^{-m_p^{-2}F(\tau)}W(\tau) \end{cases} , \tag{4.1.8}$$

where $F(\tau)$ is a function of τ. We use a unit $m_p = 1$ for hereafter. One can find that the following Kähler potential realizes the Kähler invariance under the modular transformation:

$$K(\tau,\bar{\tau}) = -n\ln(-i\tau + i\bar{\tau}), \tag{4.1.9}$$

with positive integer n. The function $F(\tau)$ is determined to be $F = \ln(c\tau+d)^n$. Then, the modular transformation of W is

$$W(\tau) \longrightarrow (c\tau+d)^{-n}W(\tau). \tag{4.1.10}$$

The modular transformation for the chiral supermultiplet φ^I is found to be

$$\varphi^I(\tau) \longrightarrow (c\tau+d)^{-k_I}\rho^I(\gamma)\varphi^I(\tau), \tag{4.1.11}$$

where $\rho^I(\gamma)$ is a representation matrix of $\gamma \in \Gamma_N$ and k_I a real parameter called as the weight. The supergravity Lagrangian G is invariant if the following condition is satisfied:

$$\rho_m(\gamma)\prod_{I=1}^{I_m}\rho^I_m(\gamma) \ni \mathbf{1}, \quad \text{and} \quad \sum_{I=1}^{I_m} k_I = k_m - n, \tag{4.1.12}$$

for all couplings in the superpotential

$$W(\tau) = f_1(\tau)\varphi_1^1(\tau)\varphi_1^2(\tau)\dots\varphi_1^{I_1}(\tau) + f_2(\tau)\varphi_2^1(\tau)\varphi_2^2(\tau)\dots\varphi_2^{I_2}(\tau) + \cdots , \tag{4.1.13}$$

where k_m is the weight and $\rho_m(\gamma)$ is a representation along with the modular transformation for the coupling $f_m(\tau)$.

In $N=1$ global supersymmetry, the Kähler potential and superpotential ane disconnected in the action. The superpotential should be invariant under the modular transformation, which changes the modular invariant condition Eq. (4.1.12) into

$$\rho_m(\gamma)\prod_{I=1}^{I_m}\rho^I_m(\gamma) \ni \mathbf{1}, \quad \text{and} \quad \sum_{I=1}^{I_m} k_I = k_m. \tag{4.1.14}$$

We have assumed the coupling f_m to be a function of τ so that transforms as

$$f_m(\tau) \longrightarrow (c\tau+d)^{k_m}\rho(\gamma)f_m(\tau). \tag{4.1.15}$$

Some holomorphic functions which transforms as Eq. (4.1.15) under the Γ_N with weight 2 have been obtained for $\Gamma_2 \simeq S_3$, $\Gamma_3 \simeq A_4$, $\Gamma_4 \simeq S_4$, $\Gamma_5 \simeq A_5$ and for larger groups,

$\Delta(96)$ and $\Delta(384)$. They are called as the modular forms with weight 2. In Appendix A, we review a derivation of the modular forms for $\Gamma_3 \simeq A_4$.

The modular transformation of the chiral supermultiplet Eq. (4.1.11) allows additional modular invariant terms to the Kähler potenial as:

$$K(\tau, \bar{\tau}) = -n \ln(-i\tau + i\bar{\tau}) + \sum_I \frac{|\varphi^I(\tau)|^2}{(-i\tau + i\bar{\tau})^{k_I}}. \tag{4.1.16}$$

The VEV of τ induces the kinetic terms of the chiral supermultiplets:

$$\mathcal{L}_{kin} = \sum_I \frac{|\partial_\mu \varphi^I(\tau)|^2}{\langle -i\tau + i\bar{\tau}\rangle^{k_I}}, \tag{4.1.17}$$

which is modular invariant. A proper rescaling of the chiral supermultiplets, or alternatively redefinition of superpotential parameters in a given model, realizes a canonical form of the kinetic term under the modular transformation, which will be discussed later.

Supersymmetry should be broken and its breaking energy scale is expected to be between $\mathcal{O}(1)$ TeV and the compactification scale. The modular symmetry is broken by the VEV of τ at the compactification scale, the Planck scale or slightly lower scale.

4.2 Modular invariant model of flavor symmetry

We show some concrete models invariant under $\Gamma_3 \simeq A_4$ modular transformation in order to discuss the mechanism of flavor mixing in the lepton sector. These models are supersymmetric because we consider the modular symmetry in superstring theory. For simplicity, we discuss $N = 1$ global supersymmetric theory:

$$S = \int d^4x s^2\theta d^2\bar{\theta} K(\tau, \bar{\tau}) + \int d^4x d^2\theta W(\tau) + \text{h.c.} \tag{4.2.1}$$

We show 4 different models and their phenomenological implications. They are classsfied as follows:

I(a) : Type I seesaw model

I(b) : Type I seesaw model of an alternative theory

II : Weinberg operator model without right-handed neutrinos

III : Dirac neutrino model

4.2.1 Basic setup

At first, we show our setup based on **I(a)** model as well as **I(b)**. We assume the neutrinos to be Majorana particles and introduce three right-handed Majorana neutrinos of SU(2) singlet. The three right-handed neutrinos are combined in a triplet representation of A_4

composed by three chiral superfields as $(\nu_R)^T = (\nu_{R1}, \nu_{R2}, \nu_{R3})$. We suppose the weight of ν_R to be one, which leads to the following modular transformation:

$$\nu_R \longrightarrow (c\tau + d)^{-1}\rho(\gamma)\nu_R, \tag{4.2.2}$$

in accordance with Eq. (4.1.11). The representation matrix $\rho(\gamma)$ for a A_4 triplet given in Appendix A is

$$\rho(S) = \frac{1}{3}\begin{pmatrix} -1 & 2 & 2 \\ 2 & -1 & 2 \\ 2 & 2 & -1 \end{pmatrix}, \quad \rho(T) = \begin{pmatrix} 1 & 0 & 0 \\ 0 & \omega & 0 \\ 0 & 0 & \omega^2 \end{pmatrix}. \tag{4.2.3}$$

We also suppose that the left-handed lepton doublets, $(l_\alpha)^T = (\nu_\alpha, \alpha)$, are described as a triplet of A_4: $L^T = (l_e, l_\mu, l_\tau)$. The weight of L is 1 or -1 for **I(a)** or **I(b)** model respectively. Then we have

$$L \longrightarrow (c\tau + d)^{\mp 1}\rho(\gamma)L, \tag{4.2.4}$$

where the upper sign denotes **I(a)** and the lower does **I(b)**. The right-handed charged leptons (e, μ, τ) are three different singlet representations of A_4 ordered as $(1, 1'', 1')$ with weight 1 or 3.

$$\begin{cases} \alpha_R \longrightarrow (c\tau + d)^{-1}\rho(\gamma)\alpha_R & \text{:I(a)} \\ \alpha_R \longrightarrow (c\tau + d)^{-3}\rho(\gamma)\alpha_R & \text{:I(b)} \end{cases} \tag{4.2.5}$$

In the basis defined in Appendix A, the representations $\rho(\gamma)$ for the three singlets of A_4 are

$$\begin{aligned} &\rho(S)_{\mathbf{1}} = 1, \quad \rho(S)_{\mathbf{1}'} = 1, \quad \rho(S)_{\mathbf{1}''} = 1 \\ &\rho(T)_{\mathbf{1}} = 1, \quad \rho(T)_{\mathbf{1}'} = \omega, \quad \rho(T)_{\mathbf{1}''} = \omega^2 \end{aligned} \tag{4.2.6}$$

One may find that there are six possible assignments for the three right-handed charged leptons by interchanges of three different A_4 singlets. It is noted that such interchanges do not affect the results for lepton mixing angles since we investigate six different basis of the charged lepton mass matrix in the above assignment.

The Higgs doublets, H_u and H_d, are supposed to be trivial singlets of A_4 with zero weights. The Dirac and Majorana mass terms are obtained by these matter fields and the Higgs fields with the coupling Y.

The coupling $Y = (Y_1, Y_2, Y_3)^T$ is a A_4 triplet which transforms as in Eq. (4.1.15) with weight 2. It is approximately obtained by use of q-expansion of $Y_i(\tau)$ as

$$Y = \begin{pmatrix} Y_1(\tau) \\ Y_2(\tau) \\ Y_3(\tau) \end{pmatrix} = \begin{pmatrix} 1 + 12q + 36q^2 + 12q^3 + \dots \\ -6q^{1/3}(1 + 7q + 8q^2 + \dots) \\ -18q^{2/3}(1 + 2q + 5q^2 + \dots) \end{pmatrix}, \qquad q = e^{2\pi i\tau}. \tag{4.2.7}$$

An exact definition of Y and its derivation are given in Appendix A. The component modular forms $Y_i(\tau)$ satisfy $Y_2^2 + 2Y_1Y_3 = 0$ [50].

The representations and modular weights for the present model particles are summarized in Tab. 1. It is remarked that we have not introduced any gauge singlet scalar fields such as flavons. It may be helpful to comment about a case where the right-handed charged leptons are compiled as a A_4 triplet. It leads to a wrong mass hierarchy of charged lepton masses.

	L	e_R, μ_R, τ_R	ν_R	H_u	H_d	Y
$SU(2)$	2	1	1	2	2	1
A_4	3	$1,\ 1'',\ 1'$	3	1	1	3
$-k_I$	-1 (1)	-1 (-3)	-1	0	0	$k=2$

Table 4.2.1: The charge assignment of $SU(2)$, A_4, and the modular weight for **I(a)** model. The assignment of **I(b)** model is realized by the alternative weight in parentheses.

Type I seesaw model: I(a) and I(b)

The modular invariant mass terms of the charged lepton w_e and the neutrino w_ν in the superpotential W are

$$w_e = \alpha[e_R H_d(LY)]_{\mathbf{1}} + \beta[\mu_R H_d(LY)]_{\mathbf{1}} + \gamma[\tau_R H_d(LY)]_{\mathbf{1}}, \tag{4.2.8}$$

$$w_\nu^{\mathbf{I(a)}} = g(\nu_R H_u LY)_{\mathbf{1}} + \Lambda(\nu_R \nu_R Y)_{\mathbf{1}}, \tag{4.2.9}$$

respectively. You will find the modular weight for each coupling vanishes. The subscription $\mathbf{1}$ denotes a A_4 trivial component of the tensor multiplication of A_4 shown in Appendix B. The parameters α, β and γ are complex in general but their complex phases are non-physical since the phases can be absorbed in the right-handed charged lepton fields with a proper redefinition. We can set these parameters to be real and they have hierarchical values determined by the observed charged lepton masses. The coupling g and Λ are constant coefficients.

We also consider an alternative assignment of the modular weight for the left-handed lepton doublet and the right-handed charged leptons, which corresponds to **I(b)** model. The left-handed lepton A_4 triplet has weight 1 and the three A_4 singlets of right-handed charged leptons have -3 [51]. It leads to another modular invariant Dirac neutrino mass term without the modular form Y:

$$w_\nu^{\mathbf{I(b)}} = g(\nu_R H_u L)_{\mathbf{1}} + \Lambda(\nu_R \nu_R Y)_{\mathbf{1}}. \tag{4.2.10}$$

The neutrino masses are given by the type I seesaw mechanism.

Other models: II and III

We refer the charge assignment where both modular weights of L and right-handed charged leptons are -1 again. We discuss the II model where neutrino masses originate from the Weinberg operator. We have the superpotential

$$w_\nu^{\mathbf{II}} = -\frac{1}{\Lambda}(H_u H_u LLY)_{\mathbf{1}} \ . \tag{4.2.11}$$

In III model, the neutrinos are assumed to be Dirac particles. The neutrino mass is derived only from Dirac mass term:

$$w_\nu^{\mathbf{III}} = g(\nu_R H_u LY)_{\mathbf{1}} \tag{4.2.12}$$

4.2.2 Charged lepton mass matrix

We show a result of expansion of w_e by use of the decomposition rule of a A_4 tensor product in Appendix B.

$$\begin{aligned}
w_e &= \alpha[e_R H_d(LY)]_{\mathbf{1}} + \beta[\mu_R H_d(LY)]_{\mathbf{1}} + \gamma[\tau_R H_d(LY)]_{\mathbf{1}} \\
&= \alpha e_R H_d(LY)_{\mathbf{1}} + \beta\mu_R H_d(LY)_{\mathbf{1'}} + \gamma\tau_R H_d(LY)_{\mathbf{1''}} \\
&= \alpha e_R H_d(L_e Y_1 + L_\mu Y_3 + L_\tau Y_2) \\
&\qquad + \beta\mu_R H_d(L_\tau Y_3 + L_e Y_2 + L_\mu Y_1) \\
&\qquad\qquad + \gamma\tau_R H_d(L_\mu Y_2 + L_\tau Y_1 + L_e Y_3),
\end{aligned} \tag{4.2.13}$$

where the A_4 charge assignment for the right-handed charged leptons are $(e_R, \mu_R, \tau_R) = (1, 1'', 1')$ in this case[1]. We can obtain a mass matrix from the charged lepton Dirac mass term as

$$M_E = v_d \mathrm{diag}[\alpha, \beta, \gamma] \begin{pmatrix} Y_1 & Y_3 & Y_2 \\ Y_2 & Y_1 & Y_3 \\ Y_3 & Y_2 & Y_1 \end{pmatrix}_{RL}, \tag{4.2.14}$$

where v_d is the VEV of H_d.

4.2.3 Neutrino mass matrix

We discuss the neutrino mass matices for our present models.

Dirac neutrino mass matrix

The Dirac neutrino mass for **I(a)** and Ⅲ is decomposed as:

$$\begin{aligned}
&g(\nu_R H_u LY)_{\mathbf{1}} \\
&= v_u \left[\begin{pmatrix} \nu_{R1} \\ \nu_{R2} \\ \nu_{R3} \end{pmatrix}_{\mathbf{3}} \otimes \left[g_1 \begin{pmatrix} 2\nu_e Y_1 - \nu_\mu Y_3 - \nu_\tau Y_2 \\ 2\nu_\tau Y_3 - \nu_e Y_2 - \mu Y_1 \\ 2\nu_\mu Y_2 - \nu_\tau Y_1 - \nu_e Y_3 \end{pmatrix}_{\mathbf{3}} \oplus g_2 \begin{pmatrix} \nu_\mu Y_3 - \nu_\tau Y_2 \\ \nu_e Y_2 - \nu_\mu Y_1 \\ \nu_\tau Y_1 - \nu_e Y_3 \end{pmatrix}_{\mathbf{3}} \right] \right]_{\mathbf{1}} \\
&= v_u g_1 [\nu_{R1}(2\nu_e Y_1 - \nu_\mu Y_3 - \nu_\tau Y_2) \\
&\qquad + \nu_{R2}(2\nu_\mu Y_2 - \nu_\tau Y_1 - \nu_e Y_3) \\
&\qquad\quad + \nu_{R3}(2\nu_\tau Y_3 - \nu_e Y_2 - \nu_\mu Y_1)] \\
&\quad + v_u g_2 \left[\nu_{R1}(\nu_\mu Y_3 - \nu_\tau Y_2) + \nu_{R2}(\nu_\tau Y_1 - \nu_e Y_3) + \nu_{R3}(\nu_e Y_2 - \nu_\mu Y_1)\right],
\end{aligned} \tag{4.2.15}$$

[1] There are six possible assignment of A_4 singlets for the right-handed charged leptons such as $(e_R, \mu_R, \tau_R) = (1, 1'', 1')$, $(1, 1', 1'')$, $(1', 1, 1'')$, $(1', 1'', 1)$, $(1'', 1', 1)$, $(1'', 1, 1')$. These permutations leads to permutations of rows in the mass matrix. A Hermitian matrix $M_E^\dagger M_E$ is unchanged by such permutations up to re-labeling of parameters α, β and γ. It is therefore sufficient to discuss one case to investigate all the possible A_4 assignments for the right-handed charged lepton.

where the additional constant parameters g_1 and g_2 are derived from the ambiguity of the relative coefficients $\mathbf{3}_{\rm syn}$ and $\mathbf{3}_{\rm asy}$ in the decomposition rule of a A_4 tensor product. It leads to the following Dirac neutrino mass matrix

$$M_D = v_u \begin{pmatrix} 2g_1Y_1 & (-g_1+g_2)Y_3 & (-g_1-g_2)Y_2 \\ (-g_1-g_2)Y_3 & 2g_1Y_2 & (-g_1+g_2)Y_1 \\ (-g_1+g_2)Y_2 & (-g_1-g_2)Y_1 & 2g_1Y_3 \end{pmatrix}_{RL} . \tag{4.2.16}$$

For the alternative case **I(b)**, the Dirac neutrino mass term is decomposed as:

$$g(\nu_R H_u L)_{\mathbf{1}} = v_u g \begin{pmatrix} \nu_{R1} \\ \nu_{R2} \\ \nu_{R3} \end{pmatrix} \otimes \begin{pmatrix} \nu_e \\ \nu_\mu \\ \nu_\tau \end{pmatrix} = v_u g \left(\nu_{R1}\nu_e + \nu_{R2}\nu_\tau + \nu_{R3}\nu_\mu\right). \tag{4.2.17}$$

We have the Dirac neutrino mass matrix as:

$$M'_D = v_u g \begin{pmatrix} 1 & 0 & 0 \\ 0 & 0 & 1 \\ 0 & 1 & 0 \end{pmatrix}_{RL} . \tag{4.2.18}$$

For **III** case, where the neutrinos are Dirac particles, we have the neutrino mass matrix

$$M_\nu^{\mathbf{III}} = M_D \tag{4.2.19}$$

Majorana neutrino mass matrix

The mass term of the right-handed Majorana neutinos is written as

$$\begin{aligned} \Lambda(\nu_R\nu_R Y)_{\mathbf{1}} &= \Lambda \left[\begin{pmatrix} 2\nu_{R1}\nu_{R1} - \nu_{R2}\nu_{R3} - \nu_{R3}\nu_{R2} \\ 2\nu_{R3}\nu_{R3} - \nu_{R1}\nu_{R2} - \nu_{R2}\nu_{R1} \\ 2\nu_{R2}\nu_{R2} - \nu_{R3}\nu_{R1} - \nu_{R1}\nu_{R3} \end{pmatrix} \otimes \begin{pmatrix} Y_1 \\ Y_2 \\ Y_3 \end{pmatrix} \right]_{\mathbf{1}} \\ &= \Lambda \left[(2\nu_{R1}\nu_{R1} - \nu_{R2}\nu_{R3} - \nu_{R3}\nu_{R2})Y_1 + \right. \\ &\qquad (2\nu_{R3}\nu_{R3} - \nu_{R1}\nu_{R2} - \nu_{R2}\nu_{R1})Y_3 \\ &\qquad\qquad \left. + (2\nu_{R2}\nu_{R2} - \nu_{R3}\nu_{R1} - \nu_{R1}\nu_{R3})Y_2 \right]. \end{aligned} \tag{4.2.20}$$

It leads to the mass matrix as

$$M_N = \Lambda \begin{pmatrix} 2Y_1 & -Y_3 & -Y_2 \\ -Y_3 & 2Y_2 & -Y_1 \\ -Y_2 & -Y_1 & 2Y_3 \end{pmatrix}_{RR} . \tag{4.2.21}$$

For **I(a)** and **I(b)**, we have the effective neutrino mass matrices by the type I seesaw mechanism:

$$M_\nu^{\mathbf{I(a)}} = -M_D^{\rm T} M_N^{-1} M_D, \tag{4.2.22}$$

$$M_\nu^{\mathbf{I(b)}} = -(M'_D)^{\rm T} M_N^{-1} M'_D, \tag{4.2.23}$$

Model	Neutrino mass matrix
I (a)	$M_D \propto \begin{pmatrix} 2g_1Y_1 & (-g_1+g_2)Y_3 & (-g_1-g_2)Y_2 \\ (-g_1-g_2)Y_3 & 2g_1Y_2 & (-g_1+g_2)Y_1 \\ (-g_1+g_2)Y_2 & (-g_1-g_2)Y_1 & 2g_1Y_3 \end{pmatrix}, \quad M_N \propto \begin{pmatrix} 2Y_1 & -Y_3 & -Y_2 \\ -Y_3 & 2Y_2 & -Y_1 \\ -Y_2 & -Y_1 & 2Y_3 \end{pmatrix}$
I (b)	$M'_D \propto \begin{pmatrix} 1 & 0 & 0 \\ 0 & 0 & 1 \\ 0 & 1 & 0 \end{pmatrix}, \quad M_N \propto \begin{pmatrix} 2Y_1 & -Y_3 & -Y_2 \\ -Y_3 & 2Y_2 & -Y_1 \\ -Y_2 & -Y_1 & 2Y_3 \end{pmatrix}$
II	$M_\nu^{\mathbf{II}} \propto \begin{pmatrix} 2Y_1 & -Y_3 & -Y_2 \\ -Y_3 & 2Y_2 & -Y_1 \\ -Y_2 & -Y_1 & 2Y_3 \end{pmatrix}$
III	$M_\nu^{\mathbf{III}} \propto \begin{pmatrix} 2g_1Y_1 & (-g_1+g_2)Y_3 & (-g_1-g_2)Y_2 \\ (-g_1-g_2)Y_3 & 2g_1Y_2 & (-g_1+g_2)Y_1 \\ (-g_1+g_2)Y_2 & (-g_1-g_2)Y_1 & 2g_1Y_3 \end{pmatrix}$

Table 4.2.2: The classification of the modular invariant mass matrices for neutrino models.

The Majorana masses originate from the Weinberg operator in Eq.(4.2.11) is decomposed as:

$$\begin{aligned} w_\nu &= -\frac{v_u^2}{\Lambda}\begin{pmatrix} 2\nu_e\nu_e - \nu_\mu\nu_\tau - \nu_\tau\nu_\mu \\ 2\nu_\tau\nu_\tau - \nu_e\nu_\mu - \nu_\mu\nu_\tau \\ 2\nu_\mu\nu_\mu - \nu_\tau\nu_e - \nu_e\nu_\tau \end{pmatrix} \otimes \begin{pmatrix} Y_1 \\ Y_2 \\ Y_3 \end{pmatrix} \\ &= -\frac{v_u^2}{\Lambda}[(2\nu_e\nu_e - \nu_\mu\nu_\tau - \nu_\tau\nu_\mu)Y_1 + (2\nu_\tau\nu_\tau - \nu_e\nu_\mu - \nu_\mu\nu_e)Y_3 + \\ &\qquad (2\nu_\mu\nu_\mu - \nu_\tau\nu_e - \nu_e\nu_\tau)Y_2]. \end{aligned} \tag{4.2.24}$$

The Majorana neutrino mass matrix is given as follows:

$$M_\nu^{\mathbf{II}} = -\frac{v_u^2}{\Lambda}\begin{pmatrix} 2Y_1 & -Y_3 & -Y_2 \\ -Y_3 & 2Y_2 & -Y_1 \\ -Y_2 & -Y_1 & 2Y_3 \end{pmatrix}_{LL}. \tag{4.2.25}$$

This matrix is the same one as in Eq.(4.2.21) apart from the normalization because both left-handed neutrinos and the right-handed neutrinos are the triplet of A_4. Finally, we summarize the classification of mass matrices for neutrino models in Tab. 2.

The kinetic terms of the chiral supermultiplets Eq. (4.1.17) should be canonical for the modular transformation. We can make it canonical by a proper rescaling of the matter fields, which can be reflected to a rescaling of the model parameters in the mass matrices. The canonical form is realized by the following redefinitions:

$$\begin{aligned} &\alpha \to \alpha' = \frac{\alpha}{\sqrt{K_L K_{e_R}}}, \quad \beta \to \beta' = \frac{\beta}{\sqrt{K_L K_{\mu_R}}}, \quad \gamma \to \gamma' = \frac{\gamma}{\sqrt{K_L K_{\tau_R}}}, \\ &g_i \to g'_i = \frac{g_i}{\sqrt{K_L K_{\nu_R}}}\,(i=1,2), \quad \Lambda \to \Lambda' = \frac{\Lambda}{K_{\nu_R}}, \end{aligned} \tag{4.2.26}$$

where K_ϕ denotes a coefficient of the kinetic term of Eq. (4.1.17) in front of $|\partial_\mu \phi|^2$. In the following, we use rescaled parameters α', β', γ' g_i', and Λ' without primes instead of the original superpotential parameters.

4.3 Phenomenological implications

Let us discuss the numerical predictions for the neutrino oscillation experiments from the present four models: **I(a)**, **I(b)**, **II** and **III**. These models predict three lepton mixing angles θ_{12}, θ_{23}, and θ_{13}; and two mass squared differences Δm_{21}^2 and Δm_{31}^2, which will be a crucial test whether the models are realistic or not. We have further predictions for the Dirac CP violating phase δ_{CP} which is expected to be observed precisely in the near future. We also discuss implications of Majorana neutrinos by giving predictions for the effective neutrino mass $\langle m_{ee} \rangle$ of the $0\nu\beta\beta$ decay; and the Majorana CP violating phases α_{21} and α_{31}.

4.3.1 Simulation method

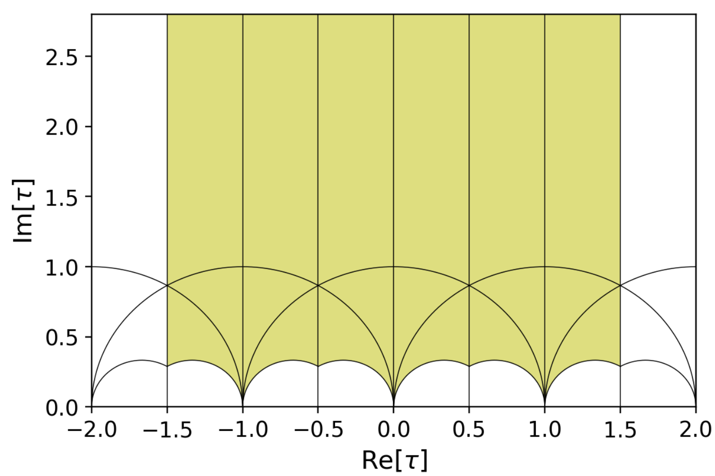

Figure 4.3.1: The fundamental domain of Γ_3 modular forms.

In order to make a realistic discussion, we constrain our models with the global fit of the neutrino oscillation experiments given from NuFIT 4.1 [3] in $3\,\sigma$ confidence level (C.L.) for the three mixing angles and two mass squared differences as summarized in Tab. 3. The models are also constrained by the observed charged lepton masses:

$$m_e = 0.5110 \text{ [MeV]}, \quad m_\mu = 105.66 \text{ [MeV]}, \quad m_\tau = 1776.86 \text{ [MeV]}, \tag{4.3.1}$$

which determines the values of α, β and γ after τ is fixed as shown in Appendix X. The cosmological observations also provide a constraint on the sum of neutrino masses [98,99]. Planck 2018 implies $m_1 + m_2 + m_3 \leq 120$–160 meV [100] at the 95% C.L., where the ambiguity of the upper bound depends on selection of combined data from several observatories. We use 160 meV for the constraint.

We survey our models for $\mathrm{Re}[\tau] \in [-1.5, 1.5]$ and $\mathrm{Im}[\tau] \in [0.1, 15]$. It is known that the modular forms describes a fundamental domain. We show the fundamental domain of Γ_3 by olive-color in Fig. 4.3.1 [50]. Any point outside of the fundamental domain corresponds to a point inside by a specific Γ_3 transformation. Therefore, it is sufficient to survey our model in the range $\mathrm{Re}[\tau] \in [-1.5, 1.5]$. The least value of $\mathrm{Im}[\tau]$ is set artificially due to computational accuracy in the numerical simulation. The maximum value is large enough to obtain the realistic mixing angles.

4.3.2 Model I(a): Seesaw

We show the phenomenological aspects of model **I(a)** numerically. We calculate the lepton mixing by use of the charged lepton mass matrix Eq. (4.2.14) and the neutrino mass matrix Eq. (4.2.22). We have two free complex parameters, the modulus τ and g_1/g_2 for our predictions. We redefine the ratio as

$$g e^{i\phi_g} \equiv \frac{g_2}{g_1}. \tag{4.3.2}$$

The phase factor ϕ_g is scanned for $[-\pi, \pi]$. The magnitude g and $\mathrm{Im}[\tau]$ will be restricted by the experimental constraint.

The experimental constraints in Tab. 3 and the cosmological upper bound for the neutrino mass, $\sum m_i < 0.16$ eV, restrict the allowed value of τ as shown by cyan points in Fig. 4.3.2. The result shows realistic predictions only for NH case, but the predicted neutrino mass is too large for IH case. The allowed regions appear along the circles and straight lines. In fact, we have made the circles and straight lines so that each point on the line is related to a point on another line by the S and T transformations. You will see that every point is related to each other by some combinations of S and T transformations. For example, we show two pairs of white- and red-colored points to see the S transformation ($S^2 = 1$). Since the theory is Γ_3 invariant, all the isolated regions predict the same physical predictions.

We have found an interesting correlation between $\sin^2\theta_{23}$ and δ_{CP} in Fig. 4.3.3. The black lines denote the experimental bounds of $\sin^2\theta_{23}$ at 3σ C.L.. The best fit value of $\sin^2\theta_{23}$ for NH: $\sin^2\theta_{23} = 0.563$, can predict $\delta_{CP} = -90^\circ$, which may be favored in the future experiments. It is also remarkable that the predicted $\sin^2\theta_{23}$ is larger than 0.544 and the magnitude of Dirac CP violating phase is predicted for $|\delta_{CP}| > 45^\circ$), which will be a test of consistency for **I(a)** model.

We note that the predicted $\sin^2\theta_{12}$ and $\sin^2\theta_{13}$ are allowed in full range of the experimental 3σ C.L..

We also show the prediction for the effective neutrino mass $\langle m_{ee}\rangle$ which will be measured in the $0\nu\beta\beta$ decay amplitude if the neutrinos are Majorana particles. One can find the predicted value of $\langle m_{ee}\rangle$ is severely limited in 21.5–23.6 [meV] in Fig. 4.3.4. It is expected that the future development of the $0\nu\beta\beta$ decay searches provide a crucial test of the model. The absolute neutrino mass scale is also predicted in a narrow range as

$38.8 < m_1 < 42.4$ [meV], which will be tested by the cosmological observations[2].

We obtain the predictions for the Majorana CP violating phases α_{21} and α_{31} in Fig. 4.3.5, which will be also measured by the $0\nu\beta\beta$ decay amplitude as Eq. (1.2.29). We will obtain a clear constraint for the Majorana CP violating phases if the absolute neutrino mass and $\langle m_{ee}\rangle$ are determined precisely. However, we have a strong predictions for these phases which require that $\alpha_{21} \sim \pm(118°–137°)$ and $\alpha_{31} \sim \pm(86°–127°)$. It also may be a test of our model in the future.

The constraints for the model parameters g and ϕ_g are shown in Figs. 4.3.6 and 4.3.7. The horizontal black lines show the experimental bounds of $\sin^2\theta_{12}$ at 3σ C.L.. We show the allowed region of ϕ_g only for $\phi_g > 0$ in order to see a correlation clearly. It is noted that the prediction is symmetric under $\phi_g \to -\phi_g$. The parameters g and ϕ_g are restricted by the experimental allowed range of $\sin^2\theta_{12}$.

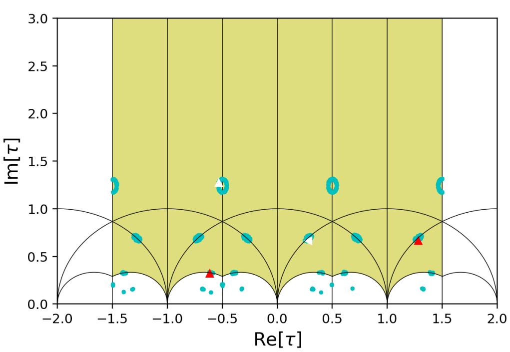

Figure 4.3.2: The allowed region of τ in **I(a)** model. The experimental 3σ C.L. is realized by NH case only.

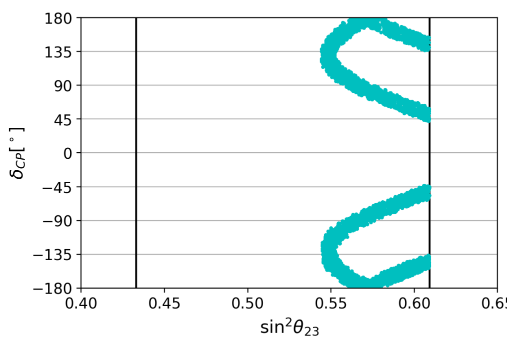

Figure 4.3.3: The prediction of $\sin^2\theta_{23}$ and δ_{CP}. The black lines represent the experimental data at 3σ C.L.. This figure is taken from [52].

4.3.3 Model I(b): Seesaw

We discuss the other seesaw model **I(b)** obtained by the alternative charge assignment [51]. The lepton mixing is obtained by diagonalization of the charged lepton mass matrix Eq. (4.2.14) and the neutrino mass matrix Eq. (4.2.23). The Dirac neutrino mass matrix Eq. (4.2.18) is a constant matrix. Thus, we have only one complex parameter τ to be fixed by the experiments. The following predictions are constrained only by the observed mass squared differences: Δm^2_{atm} and Δm^2_{sol}.

The consistent mass squared differences are reproduced by **I(b)** for both NH and IH cases by some values of τ as shown in Fig. 4.3.8. The cyan and red points denote the NH and IH cases respectively. However, these predicted regions are inconsistent to the experimental data of the mixing angles.

[2] The numerical simulation predicts the sum of neutrino masses 141–152 [meV], which is excluded if we take the most stringent upper bound for the neutrino mass 120 [meV] given from the cosmological observation.

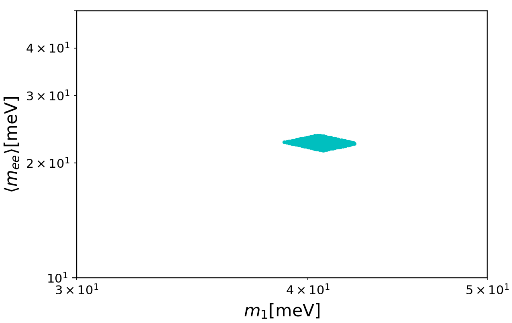

Figure 4.3.4: The prediction of m_{ee} versus m_1 for NH in model I(a). This figure is taken from [52].

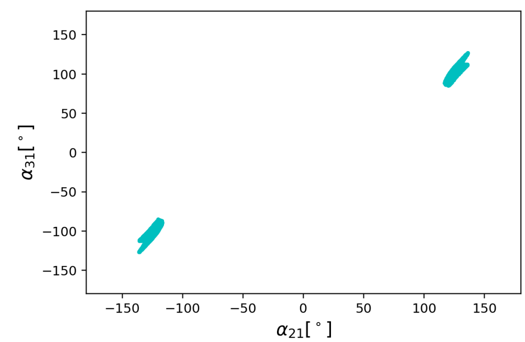

Figure 4.3.5: The prediction of Majorana phases α_{21} and α_{31} for NH in I(a). This figure is taken from [52].

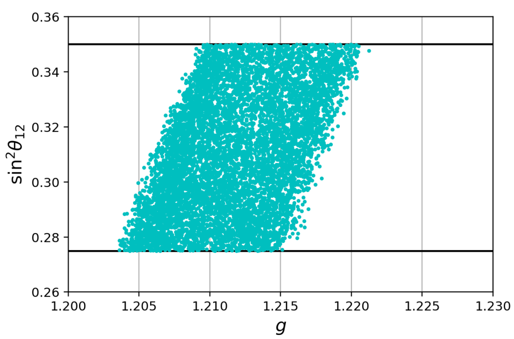

Figure 4.3.6: A correlation between g and $\sin^2\theta_{12}$. The black lines represent the experimental data at 3σ C.L..

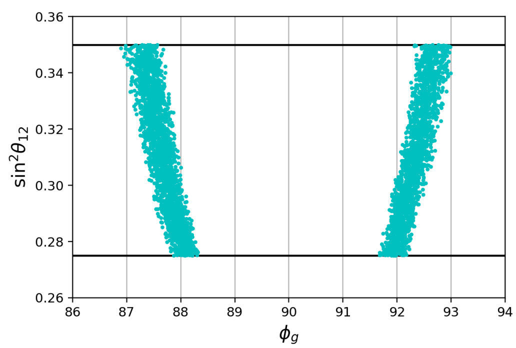

Figure 4.3.7: A correlation between ϕ_g and $\sin^2\theta_{12}$. The black lines represent the experimental data at 3σ C.L..

We show the prediction of $\sin^2\theta_{13}$ and δ_{CP} in Fig. 4.3.9. The vertical black lines denote the experimental bounds of $\sin^2\theta_{13}$ at 3σ C.L.. The predicted value of $\sin^2\theta_{13}$ is 0.18 and it is too large for NH case. On the other hand, we have $\sin^2\theta_{13} = 0$ or 1 for IH case. Both predictions are inconsistent with the experiments.

One also finds the CP violating phase in this model. For NH case, the predicted CP violating phase is $|\delta_{CP}| < 90^\circ$. For IH case, the maximal CP violation $\delta_{CP} = \pm 90^\circ$ is realized for $\theta_{13} = \pm 90^\circ$. The Dirac CP violating phase cannot be determined if there is no mixing in 1-3 plane: $\theta_{13} = 0$.

4.3.4 Model II: Weinberg operator

We also show our numerical results for **II** where the right-handed neutrinos are not introduced. The neutrino mass matrix is described by the Weinberg operator Eq. (4.2.25), while the charged lepton mass matrix is again Eq. (4.2.14). Only the modulus parameter

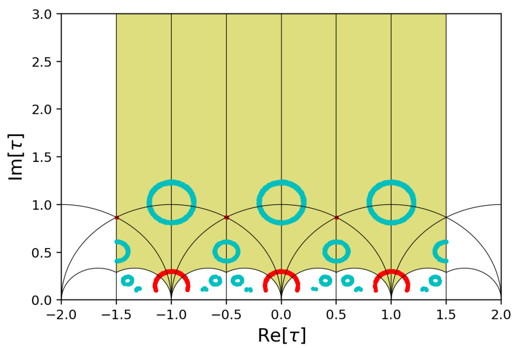

Figure 4.3.8: The allowed values of τ for **I(b)** which satisfy the observed neutrino mass squared differences at 3σ C.L..

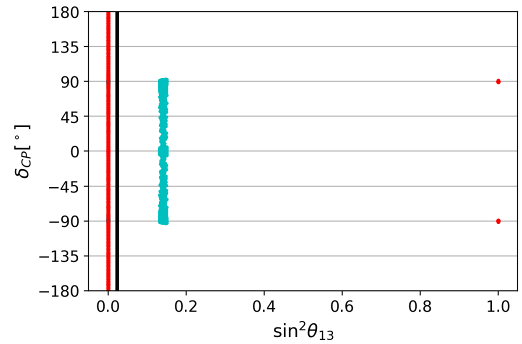

Figure 4.3.9: The prediction $\sin^2\theta_{13}$ and δ_{CP}. The black lines represent the experimental data at 3σ C.L.. Both NH and IH cases are excluded.

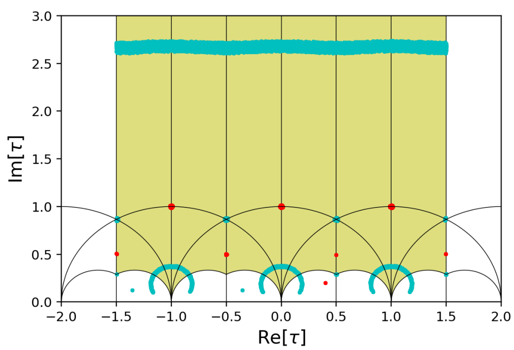

Figure 4.3.10: The allowed values of τ for **II** which satisfy the obsrved neutrino mass squared differences at 3σ C.L..

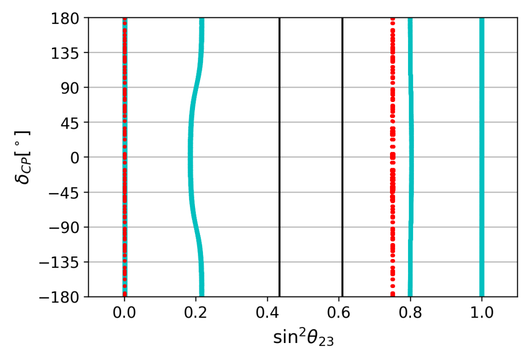

Figure 4.3.11: The prediction $\sin^2\theta_{23}$ and δ_{CP}. The black lines represent the experimental data at 3σ C.L..

τ is the free parameter which contributes to the flavor mixing. We show the prediction of this model taking account of the constraint from the observed mass squared differences: Δm^2_{atm} and Δm^2_{sol}.

The modulus τ is constrained as in Fig. 4.3.10. The cyan and red points denote the NH and IH cases respectively. The allowed regions of τ cannot reproduce the experimental data of the mixing angles.

The prediction of $\sin^2\theta_{23}$ and δ_{CP} are shown in Fig. 4.3.11. The vertical black lines denote the experimental bounds of $\sin^2\theta_{23}$ at 3σ C.L.. We have $\sin^2\theta_{23} \sim 0$, 0.2, 0.8 or 1 for NH case. In IH case, the predicted θ_{23} implies $\sin^2\theta_{23} \sim 0$ or 0.7. Then, the predicted values of $\sin^2\theta_{23}$ are all outside of the observed 3σ C.L. for both NH and IH case. The Dirac CP violating phase cannot be determined: $\delta_{CP} \in [-180°, 180°]$.

4.3.5 Model III: Dirac neutrino

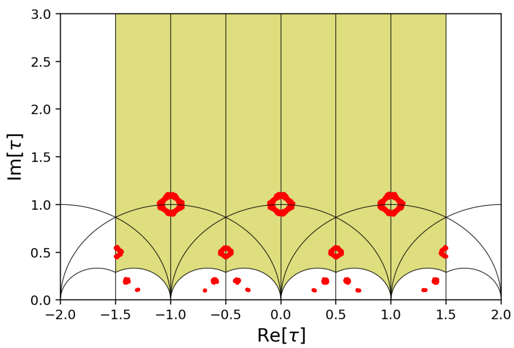

Figure 4.3.12: The allowed region of τ in **III** model. The IH case is only allowed by the current experiments.

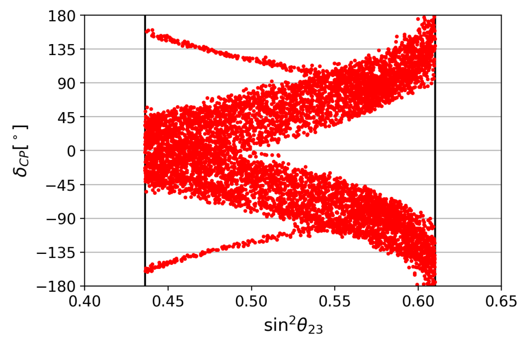

Figure 4.3.13: The prediction of $\sin^2\theta_{23}$ and δ_{CP}. The black lines represent the experimental data with 3σ C.L.. This figure is taken from [52].

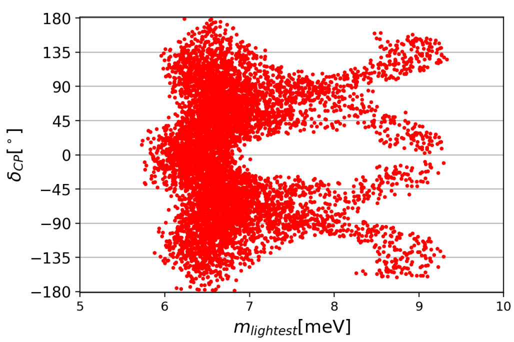

Figure 4.3.14: The prediction of the lightest neutrino mass and δ_{CP}.

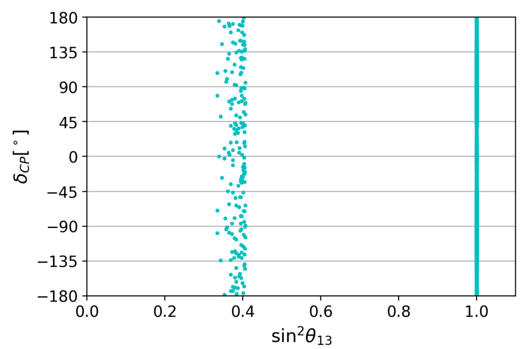

Figure 4.3.15: The prediction of $\sin^2\theta_{13}$ in terms of δ_{CP} for NH.

We discuss the model **III** where the neutrinos are assumed to be Dirac particles. The neutrino mass matrix is obtained as the Dirac mass terms Eq. (4.2.19). We use the charged lepton mass matrix of Eq. (4.2.14).

We have found that this model is consistent to the observed experimental results of the three mixing angles and two mass squared differences for IH. We show the allowed regions of τ in the complex plane in Fig. 4.3.12. Each isolated region moves to another allowed region with the corresponding combination of Γ_3 transformations. The same predictions will be obtained from all the isolated regions.

The predictions of the three mixing angles are as wide as the corresponding observed ranges with 3σ C.L. of the global fit. The predicted Dirac CP violating phase δ_{CP} is not constrained by the current observation. However, we have an interesting correlation

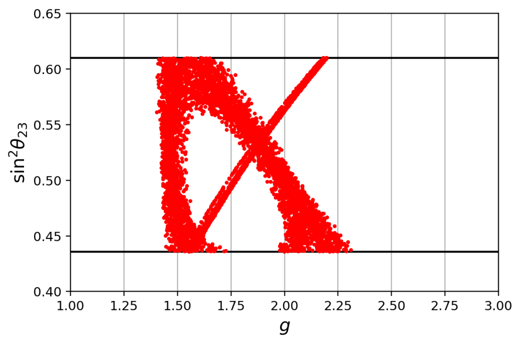

Figure 4.3.16: The allowed g in terms of $\sin^2\theta_{23}$.

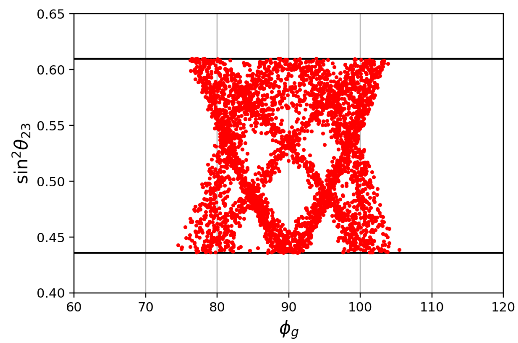

Figure 4.3.17: The correlation between ϕ_g and $\sin^2\theta_{23}$.

between $\sin^2\theta_{23}$ and δ_{CP} as shown in Fig. 4.3.13. The black lines represents the upper and lower bound of the global fit at 3σ C.L.. One finds that the best fit $\sin^2\theta_{23} = 0.563$ and maximal CP violation $|\delta_{CP}| = 90°$ can be realized. It is also remarkable that the model can be excluded if ,for example, the future development in the measurement of CP violation observes $\delta_{CP} < -120°$ near the best fit of $\sin^2\theta_{23}$.

This model also gives a strong prediction for the absolute mass of the neutrino. The lightest neutrino mass eigenvalue is shown with the prediction of δ_{CP} in Fig. 4.3.14. The prediction implies $5.73 < m_3 < 9.33$ [meV]. The sum of neutrino masses is predicted as $104 < \sum m_i < 112$ [meV], which is expected to be tested by the cosmological observation in the near future. The correlation between the mass and δ_{CP} implies that it will be possible to exclude this model if, for example, the future precise measurement reveals that the lightest neutrino mass is about 8 [meV] and the Dirac CP phase is less than $-120°$ for IH.

For NH case, we have a wrong prediction for θ_{13} obtained by the constraints of θ_{12}, θ_{23} and the two mass squared differences as shown in Fig. 4.3.15. The predicted $\sin^2\theta_{13}$ is too large: $\sin^2\theta_{13} \sim 0.4$ or 1.

The successful predictions for IH case is obtained by the model parameter g and ϕ_g in addition to τ. The allowed value of g is constrained by the observed θ_{23} for $1.40 < g < 2.31$ as in Fig. 4.3.16. We also have a constraint for ϕ_g from θ_{23}: $74.8° < |\phi_g| < 115°$ as shown in Fig. 4.3.17. The horizontal black lines in these figure denote the experimental bounds of $\sin^2\theta_{23}$ at 3σ C.L..

Comments on Figures in 4.3

The figures 4.3.3, 4.3.4, 4.3.5 and 4.3.13 are taken from [52] including some changes. We note the changes in these figures.

- The experimental data are updated. We have used NuFIT 4.1 (2019) in the thesis instead of NuFIT 3.2 (2018).

- We have investigated wider values of Im[τ]. The lowest value is reduced to 0.1 from 0.6.
- We scan the input value of Δm^2_{atm} within 3σ C.L. in the thesis. The bestfit value is used as the input value in [52].

4.4 Chapter summary

We have discussed the phenomenological aspects of the modular invariant models with A_4 symmetry. Our numerical simulations have provided clear predictions in terms of the given four models, and two of them are found to be realistic, which will encourage us to explore other modular symmetric models.

We have investigated the two kinds of type I seesaw models (**I(a)** and **I(b)**), Weinberg operator model (**II**) and Dirac neutrino model (**III**). These models have no additional scalar fields such as flavons. The degrees of freedom in the lepton mixing are the modulus parameter τ, and a complex parameter g for **I(a)** and **III**, apart from interchanges of the hierarchical values of α, β and γ which are determined by the charged lepton masses.

We have investigated those four models with sufficiently wide τ and g for all interchanges of α, β and γ; and it is found that the normal hierarchy of neutrino masses is realized in **I(a)** model and the inverted hierarchy is possible in **III** model. These models are consistent to the current experimental data of NuFIT 4.1 [3] and the cosmological upper bound on the neutrino masses [100]. The models **I(b)** and **III** must be extended.

We have obtained a strong prediction from **I(a)** model for NH case. The predicted correlation of $\sin^2\theta_{23}$ and δ_{CP} will be testable in the future experiments of the neutrino oscillations. The predicted region of $\langle m_{ee}\rangle$ is also narrow, and it will be tested by the future $0\nu\beta\beta$ searches. The sum of neutrino masses is also given in a narrow range, which may be excluded by the further cosmological observation.

The Dirac neutrinos are possible in **III** model for IH case.

One may think that the effects from the supersymmetry breaking and the renormalization corrections change our numerical results. In Ref. [51], one finds that the SUSY breaking effect can be neglected if the SUSY breaking scale is much smaller than the mass of the mediator connecting the visible sector and softly SUSY breaking sector. One also finds a careful discussion in the same reference for the radiative corrections for both the type I seesaw and Weinberg operator models; and such effects are negligible for small $\tan\beta$.

It is also important to find a mechanism which determines the value of τ. This is a problem called the modular stabilization. One can find an approach to the problem in supergravity theory [105, 106].

Chapter 5

Conclusion

We have presented some phenomenological discussions for the lepton flavor mixing. The desired improvement to the SM for massive neutrinos must be consistent to the neutrino oscillation experiments. The flavor symmetry may be a powerful candidate to explain the flavor mixing. We have shown the typical three approaches, flavor symmetry, texture zeros and modular symmetry by use of our models.

In chapter 2, We have reviewed A_4 and Z_3 flavor symmetry model [27]. The charged lepton mass hierarchy and the neutrino mixing are explained by the VEVs of flavons introduced in addition to the Higgs fields. A successful VEV alignment has been obtained by the potential analysis. Our numerical simulation has provided clear correlations among the observable and the model parameters. We have found that the predictions of the three mixing angle and the Dirac CP violating phase are consistent to the global fit in 1σ C.L.. It is remarked that the results may be favored for the future development of the neutrino oscillation experiments.

In chapter 3, we have discussed a minimal texture of the neutrino mass matrix [47]. The texture zeros approach is useful to search for the minimal flavor model. It is important to discuss both top-down approach and bottom-up approach in a phenomenological point of view. Our minimal texture introduces two right-handed Majorana neutrinos and leads to 3×2 Dirac neutrino mass matrix, which is realized S_4 flavor symmetry. We have obtained a minimal texture where the mixing parameters, effective mass $\langle m_{ee} \rangle$ and Majorana CP violating phases are determined only by k and ϕ_B after we fix the other two parameters with the neutrino mass squared differences. The results are very limited especially for the Dirac CP violating phase. We can distinguish the sign of δ_{CP} by values of k and ϕ_B. A further discussion in Ref [104] has shown $\sin \phi_B > 0$ due to the cosmological observation of BAU.

In chapter 4, We have presented a new approach where the Yukawa couplings are described by the modular forms. The theory has a modular symmetry which can be the origin of the flavor symmetry. This approach does not require a SU(2) gauge singlet scalar field such as flavon. Since the values of modular forms are determined by the modulus τ, a modular symmetric model can be minimal. We have reviewed a set up for the modular invariant flavor theory and presented our recent work [52] where $\Gamma_3 \simeq A_4$ invariance is assumed. We have performed numerical simulations for four models obtained from different scenarios to induce finite neutrino masses. For the two realistic models, we can freely fix two complex parameters to obtain the three mixing angles and two mass squared differences. On the other hand, the other models have only a free parameter τ and they are found to be unrealistic. In Refs. [105, 106], We have also discussed the modular stabilization in order to find a mechanism to fix τ.

Acknowledgement

I would like to thank my parents for their infinite kindness and love. I also thank my supervisor Prof. Takuya Morozumi for useful discussions and grateful encouragements. I also thank Prof. Morimitsu Tanimoto, Prof. Tatsuo Kobayashi and Dr. Yusuke Shimizu for their kind lectures and useful discussions. I also thank my family, my friends, my colleagues and the members of physics office for their help in my daily life.

Appendix A

Transformation and multiplication rule

We show the multiplication rule of A_4 group. We have several representations for A_4 group of orders $\mathbf{1}$, $\mathbf{1}'$, $\mathbf{1}''$ and $\mathbf{3}$. These A_4 representations are transformed by S and T:

$$\begin{aligned}
\mathbf{1}\ &: S(\mathbf{1}) = 1, \qquad T(\mathbf{1}) = 1, \\
\mathbf{1}'\ &: S(\mathbf{1}') = 1, \qquad T(\mathbf{1}') = \omega, \\
\mathbf{1}''\ &: S(\mathbf{1}'') = 1, \qquad T(\mathbf{1}'') = \omega^2, \\
\mathbf{3}\ &: S(\mathbf{3}) = \frac{1}{3}\begin{pmatrix} -1 & 2 & 2 \\ 2 & -1 & 2 \\ 2 & 2 & -1 \end{pmatrix}, \quad T(\mathbf{3}) = \begin{pmatrix} 1 & 0 & 0 \\ 0 & \omega & 0 \\ 0 & 0 & \omega^2 \end{pmatrix}.
\end{aligned} \tag{A.0.1}$$

They satisfy the following condition:

$$S(\boldsymbol{r})^2 = T(\boldsymbol{r})^3 = (S(\boldsymbol{r})T(\boldsymbol{r}))^3 = 1, \tag{A.0.2}$$

for each order $\boldsymbol{r}$. Multiplications of two A_4 representations obey the following rule:

$$\begin{gathered}
\mathbf{1}\otimes\mathbf{1} = \mathbf{1}'\otimes\mathbf{1}'' = \mathbf{1}''\otimes\mathbf{1}' = \mathbf{1} \\
\mathbf{1}\otimes\mathbf{1}' = \mathbf{1}'\otimes\mathbf{1} = \mathbf{1}''\otimes\mathbf{1}'' = \mathbf{1}' \\
\mathbf{1}\otimes\mathbf{1}'' = \mathbf{1}''\otimes\mathbf{1} = \mathbf{1}'\otimes\mathbf{1}' = \mathbf{1}'' \\
\mathbf{1}\otimes\mathbf{3} = \mathbf{3}\otimes\mathbf{1} = \mathbf{1}'\otimes\mathbf{3} = \mathbf{3}\otimes\mathbf{1}' = \mathbf{1}''\otimes\mathbf{3} = \mathbf{3}\otimes\mathbf{1}'' = \mathbf{3}
\end{gathered} \tag{A.0.3}$$

The multiplication between two representations of order $\mathbf{3}$ (triplets) is reducible:

$$\mathbf{3}\otimes\mathbf{3} = \mathbf{1}\oplus\mathbf{1}'\oplus\mathbf{1}''\oplus\mathbf{3}_{\mathrm{S}}\oplus\mathbf{3}_{\mathrm{A}}, \tag{A.0.4}$$

where $\mathbf{3}_{\mathrm{S}}$ and $\mathbf{3}_{\mathrm{A}}$ components are symmetric (commutable) and anti-symmetric (ant-commutable) in the multiplication respectively. The multiplication of triplets is written as:

$$
\begin{aligned}
\begin{pmatrix} a_1 \\ a_2 \\ a_3 \end{pmatrix}_{\mathbf{3}} \otimes \begin{pmatrix} b_1 \\ b_2 \\ b_3 \end{pmatrix}_{\mathbf{3}} &= (a_1b_1 + a_2b_3 + a_3b_2)_{\mathbf{1}} \oplus (a_3b_3 + a_1b_2 + a_2b_1)_{\mathbf{1'}} \\
&\oplus (a_2b_2 + a_1b_3 + a_3b_1)_{\mathbf{1''}} \\
&\oplus \frac{1}{3}\begin{pmatrix} 2a_1b_1 - a_2b_3 - a_3b_2 \\ 2a_3b_3 - a_1b_2 - a_2b_1 \\ 2a_2b_2 - a_1b_3 - a_3b_1 \end{pmatrix}_{\mathbf{3}} \oplus \frac{1}{2}\begin{pmatrix} a_2b_3 - a_3b_2 \\ a_1b_2 - a_2b_1 \\ a_3b_1 - a_1b_3 \end{pmatrix}_{\mathbf{3}},
\end{aligned}
\tag{A.0.5}
$$

where each coefficient is a convention and cannot be determined in general. The derivation is shown in the review [9, 10].

Appendix B

The derivation of modular forms

We show a derivation of the modular form of weight 2 in a $\Gamma_3 \simeq A_4$ invariant theory. We consider a general modular form:

$$f_i(\tau) \longrightarrow (c\tau + d)^{k_i} f_i(\tau), \tag{B.0.1}$$

for the modular transformation, $\tau \to (a\tau + b)/(c\tau + d)$. One can also obtain the following modular transformation:

$$Y(\tau) \equiv \frac{d}{d\tau} \sum_i \log f_i^{p_i}(\tau) \longrightarrow (c\tau + d)^2 \frac{d}{d\tau} \sum_i \log f_i^{p_i}(\tau) + c(c\tau + d) \sum_i p_i k_i, \tag{B.0.2}$$

where p_i is an arbitrary factor. The function $Y(\tau)$ is a modular form of weight 2 if $\sum p_i k_i = 0$. The Dedekind eta function is useful to obtain the modular form Eq. (4.1.15) with $k = 2$:

$$\eta(\tau) = q^{1/24} \prod_{n=1}^{\infty} (1 - q^n), \quad q = e^{2\pi i \tau}, \quad (\mathrm{Im}\tau > 0), \tag{B.0.3}$$

since we have the following property:

$$\eta(-1/\tau) = \sqrt{-i\tau}\, \eta(\tau), \quad \eta(\tau + 1) = e^{i\pi/12} \eta(\tau). \tag{B.0.4}$$

It is noted that η^{24} is a modular form of weight 12. It is also an important fact that some specific sets of the Dedekind eta functions are closed under the modular transformation. We show a closure used for $\Gamma_3 \simeq A_4$ case:

$$\begin{gathered} \eta(3\tau) \to e^{i\pi/4} \eta(3\tau) \\ \eta\left(\frac{\tau}{3}\right) \to \eta\left(\frac{\tau+1}{3}\right), \quad \eta\left(\frac{\tau+1}{3}\right) \to \eta\left(\frac{\tau+2}{3}\right), \quad \eta\left(\frac{\tau+2}{3}\right) \to e^{i\pi/12} \eta\left(\frac{\tau}{3}\right), \end{gathered} \tag{B.0.5}$$

under T transformation, $\tau \to \tau + 1$. We also have a closure under S transformation, $\tau \to -1/\tau$:

$$\begin{gathered} \eta(3\tau) \to \frac{1}{\sqrt{3}} \sqrt{-i\tau}\, \eta\left(\frac{\tau}{3}\right), \quad \eta\left(\frac{\tau}{3}\right) \to \sqrt{3}\sqrt{-i\tau}\, \eta(3\tau) \\ \eta\left(\frac{\tau+1}{3}\right) \to e^{-\pi i/12} \sqrt{-i\tau}\, \eta\left(\frac{\tau+2}{3}\right), \quad \eta\left(\frac{\tau+2}{3}\right) \to e^{\pi i/12} \sqrt{-i\tau}\, \eta\left(\frac{\tau+1}{3}\right). \end{gathered} \tag{B.0.6}$$

The above interchanges of Dedekind eta functions realize the A_4 transformation along with the modular group. We can obtain a modular form of weight 2 by use of the closed set of Dedekind eta functions:

$$Y(\alpha,\beta,\gamma,\delta|\tau) = \frac{d}{d\tau}\left[\alpha\log\eta\left(\frac{\tau}{3}\right) + \beta\log\eta\left(\frac{\tau+1}{3}\right) + \gamma\log\eta\left(\frac{\tau+2}{3}\right) + \delta\log\eta\left(3\tau\right)\right], \tag{B.0.7}$$

where $\alpha+\beta+\gamma+\delta=0$. We note that the $\sqrt{3}$ factors and phase factors appear by the transformation within the logarithmics but they have been eliminated by derivative in terms of τ. One can find interchanges of the coefficients α,β,γ and δ by S and T transformation:

$$Y(\alpha,\beta,\gamma,\delta|\tau) \longrightarrow \begin{cases} \tau^2 Y(\delta,\gamma,\beta,\alpha|\tau) & : S \\ Y(\gamma,\alpha,\beta,\delta|\tau) & : T \end{cases} \tag{B.0.8}$$

We can obtain a triplet representation $Y^{(3)}(\tau) = (Y_1(\tau), Y_2(\tau), Y_3(\tau))^T$ along with A_4 by choosing a proper values for α,β,γ and δ. We use the following setup in this thesis:

$$\begin{aligned} Y_1(\tau) &= \frac{i}{2\pi}\left(\frac{\eta'(\tau/3)}{\eta(\tau/3)} + \frac{\eta'((\tau+1)/3)}{\eta((\tau+1)/3)} + \frac{\eta'((\tau+2)/3)}{\eta((\tau+2)/3)} - \frac{27\eta'(3\tau)}{\eta(3\tau)}\right), \\ Y_2(\tau) &= \frac{-i}{\pi}\left(\frac{\eta'(\tau/3)}{\eta(\tau/3)} + \omega^2\frac{\eta'((\tau+1)/3)}{\eta((\tau+1)/3)} + \omega\frac{\eta'((\tau+2)/3)}{\eta((\tau+2)/3)}\right), \\ Y_3(\tau) &= \frac{-i}{\pi}\left(\frac{\eta'(\tau/3)}{\eta(\tau/3)} + \omega\frac{\eta'((\tau+1)/3)}{\eta((\tau+1)/3)} + \omega^2\frac{\eta'((\tau+2)/3)}{\eta((\tau+2)/3)}\right), \end{aligned} \tag{B.0.9}$$

where $\omega = e^{2\pi i/3}$. The common overall coefficient of Y_1, Y_2 and Y_3 cannot be determined. The A_4 transformation is realized along with the modular transformation as

$$Y^{(3)}(\tau) \longrightarrow \begin{cases} \tau^2\rho(S)Y^{(3)}(\tau) & : S \\ \rho(T)Y^{(3)}(\tau) & : T \end{cases} \tag{B.0.10}$$

with a specific basis of A_4 group:

$$\rho(S) = \frac{1}{3}\begin{pmatrix} -1 & 2 & 2 \\ 2 & -1 & 2 \\ 2 & 2 & -1 \end{pmatrix}, \quad \rho(T) = \begin{pmatrix} 1 & 0 & 0 \\ 0 & \omega & 0 \\ 0 & 0 & \omega^2 \end{pmatrix}. \tag{B.0.11}$$

Appendix C

Three flavor mixing of neutrinos

The flavor eigenstates of neutrinos ν_α ($\alpha = e, \mu, \tau$) are related to their mass eigenstates ν_i ($i = 1, 2, 3$) by the following unitary transformation:

$$|\nu_\alpha\rangle = \sum_{i=1}^{3} U_{\alpha i}|\nu_i\rangle, \qquad |\nu_i\rangle = \sum_{\alpha=e}^{\tau} (U^\dagger)_{i\alpha}|\nu_\alpha\rangle. \tag{C.0.1}$$

The time evolution of neutrino flavor eigenstate after a time duration t is given as

$$\begin{aligned} |\nu_\alpha\rangle_t &= \sum_{i=1}^{3} U_{\alpha i} e^{-iE_i t}|\nu_i\rangle_{t=0} \\ &= \sum_{i=1}^{3}\sum_{\gamma=e}^{\tau} U_{\alpha i} e^{-iE_i t}(U^\dagger)_{i\gamma}|\nu_\gamma\rangle_{t=0}. \end{aligned} \tag{C.0.2}$$

The transition amplitude of two different flavor states is given by

$$\begin{aligned} \mathcal{A}(t) &= {}_{t=0}\langle\nu_\beta|\nu_\alpha\rangle_t \\ &= \sum_{i=1}^{3}\sum_{\gamma=e}^{\tau} U_{\alpha i} e^{-iE_i t}(U^\dagger)_{i\gamma}\delta_{\beta\gamma} \\ &= \sum_{i=1}^{3} U_{\alpha i} e^{-iE_i t} U^*_{\beta i}. \end{aligned} \tag{C.0.3}$$

For light neutrinos, we can approximate $E_i = \sqrt{p^2 + m_i^2} \sim p + m_i^2/2p \sim p + m_i^2/2E$. We use a new dimensionless factor $t_i \equiv m_i^2 t/2E$ in the following. The transition probability from $|\nu_\alpha\rangle_t$ to $|\nu_\beta\rangle_{t=0}$ after a time t is

$$\begin{aligned}
P(\nu_\alpha \to \nu_\beta) =& |\mathcal{A}(t)|^2 \\
=& |\sum_{i=1}^{3} U_{\alpha i} e^{-it_i} U^*_{\beta i}|^2 \\
=& \sum_{i=1}^{3} |U_{\alpha i}|^2 |U_{\beta i}|^2 \\
&+ 2\mathrm{Re}[U_{\alpha 1} U^*_{\alpha 2} U^*_{\beta 1} U_{\beta 2}] \cos(t_2 - t_1) - 2\mathrm{Im}[U_{\alpha 1} U^*_{\alpha 2} U^*_{\beta 1} U_{\beta 2}] \sin(t_2 - t_1) \\
&+ 2\mathrm{Re}[U_{\alpha 1} U^*_{\alpha 3} U^*_{\beta 1} U_{\beta 3}] \cos(t_3 - t_1) - 2\mathrm{Im}[U_{\alpha 1} U^*_{\alpha 3} U^*_{\beta 1} U_{\beta 3}] \sin(t_3 - t_1) \\
&+ 2\mathrm{Re}[U_{\alpha 2} U^*_{\alpha 3} U^*_{\beta 2} U_{\beta 3}] \cos(t_3 - t_2) - 2\mathrm{Im}[U_{\alpha 2} U^*_{\alpha 3} U^*_{\beta 2} U_{\beta 3}] \sin(t_3 - t_2).
\end{aligned} \tag{C.0.4}$$

Next, we use the following unitarity conditions of a mixing matrix:

$$|U_{\alpha 1} U^*_{\beta 1} + U_{\alpha 2} U^*_{\beta 2} + U_{\alpha 3} U^*_{\beta 3}|^2 = \delta_{\alpha\beta}, \tag{C.0.5}$$

$$U_{\alpha 1} U^*_{\beta 1} + U_{\alpha 2} U^*_{\beta 2} + U_{\alpha 3} U^*_{\beta 3} = 0 \quad \text{for} \quad \alpha \neq \beta. \tag{C.0.6}$$

The first condition can be rewritten as

$$\begin{aligned}
&\sum_{i=1}^{3} |U_{\alpha i}|^2 |U_{\beta i}|^2 \\
&\quad +2\mathrm{Re}[U_{\alpha 1} U^*_{\alpha 2} U^*_{\beta 1} U_{\beta 2}] + 2\mathrm{Re}[U_{\alpha 1} U^*_{\alpha 3} U^*_{\beta 1} U_{\beta 3}] + 2\mathrm{Re}[U_{\alpha 2} U^*_{\alpha 3} U^*_{\beta 2} U_{\beta 3}] = \delta_{\alpha\beta},
\end{aligned} \tag{C.0.7}$$

and the second condition leads to

$$\mathrm{Im}[U_{\alpha 2} U^*_{\alpha 3} U^*_{\beta 2} U_{\beta 3}] = -\mathrm{Im}[U_{\alpha 1} U^*_{\alpha 3} U^*_{\beta 1} U_{\beta 3}] = \mathrm{Im}[U_{\alpha 1} U^*_{\alpha 2} U^*_{\beta 1} U_{\beta 2}] = J_{CP}, \tag{C.0.8}$$

where J_{CP} is a CP violation measure called as the Jarlskog invariant. If CP is conserved in neutrino oscillation, the Jarlskog invariant is zero. Therefore, $P(\nu_\alpha \to \nu_\beta)$ is reduced as

$$\begin{aligned}
P(\nu_\alpha \to \nu_\beta) = \delta_{\alpha\beta} &+ 2\mathrm{Re}[U_{\alpha 1} U^*_{\alpha 2} U^*_{\beta 1} U_{\beta 2}](\cos(t_2 - t_1) - 1) \\
&+ 2\mathrm{Re}[U_{\alpha 1} U^*_{\alpha 3} U^*_{\beta 1} U_{\beta 3}](\cos(t_3 - t_1) - 1) \\
&+ 2\mathrm{Re}[U_{\alpha 2} U^*_{\alpha 3} U^*_{\beta 2} U_{\beta 3}](\cos(t_3 - t_2) - 1) \\
&- 2J_{CP} \left[\sin(t_2 - t_1) + \sin(t_1 - t_3) + \sin(t_3 - t_2)\right].
\end{aligned} \tag{C.0.9}$$

Finally, we obtain the following form:

$$\begin{aligned}P(\nu_\alpha \to \nu_\beta) = \delta_{\alpha\beta} &- 4\mathrm{Re}[U_{\alpha 1}U^*_{\alpha 2}U^*_{\beta 1}U_{\beta 2}]\sin^2\left(\frac{m_2^2 - m_1^2}{4E}t\right) \\ &- 4\mathrm{Re}[U_{\alpha 1}U^*_{\alpha 3}U^*_{\beta 1}U_{\beta 3}]\sin^2\left(\frac{m_3^2 - m_1^2}{4E}t\right) \\ &- 4\mathrm{Re}[U_{\alpha 2}U^*_{\alpha 3}U^*_{\beta 2}U_{\beta 3}]\sin^2\left(\frac{m_3^2 - m_2^2}{4E}t\right) \\ &- 2J_{CP}\left[\sin\left(\frac{m_2^2 - m_1^2}{2E}t\right) + \sin\left(\frac{m_1^2 - m_3^2}{2E}t\right) + \sin\left(\frac{m_3^2 - m_2^2}{2E}t\right)\right].\end{aligned} \tag{C.0.10}$$

Bibliography

[1] Z. Maki, M. Nakagawa and S. Sakata, Prog. Theor. Phys. **28** (1962) 870.

[2] B. Pontecorvo, Sov. Phys. JETP **26** (1968) 984 [Zh. Eksp. Teor. Fiz. **53** (1967) 1717].

[3] NuFIT 4.1 (2018), www.nu-fit.org, JHEP 01 (2019) 106, [arXiv:1811.05487 [hep-ph]].

[4] K. Abe *et al.* [T2K Collaboration], [arXiv:1707.01048 [hep-ex]].

[5] W. Morgan, "T2K Status, Results, and Plans", Talk at XXVIII International Conference on Neutrino Physics and Astrophysics, 4-9 June 2018, Heidelberg, Germany, URL: https://doi.org/10.5281/zenodo.1286751.

[6] P. Adamson *et al.* [NOvA Collaboration], Phys. Rev. Lett. **118** (2017) no.23, 231801 [arXiv:1703.03328 [hep-ex]].

[7] M. Sanchez, "NOvA Results and Prospects?", Talk at XXVIII International Conference on Neutrino Physics and Astrophysics, 4-9 June 2018, Heidelberg, Germany, URL: https://doi.org/10.5281/zenodo.1286757.

[8] G. Altarelli and F. Feruglio, Rev. Mod. Phys. **82** (2010) 2701 [arXiv:1002.0211 [hep-ph]].

[9] H. Ishimori, T. Kobayashi, H. Ohki, Y. Shimizu, H. Okada and M. Tanimoto, Prog. Theor. Phys. Suppl. **183** (2010) 1 [arXiv:1003.3552 [hep-th]].

[10] H. Ishimori, T. Kobayashi, H. Ohki, H. Okada, Y. Shimizu and M. Tanimoto, Lect. Notes Phys. **858** (2012) 1, Springer.

[11] D. Hernandez and A. Y. Smirnov, Phys. Rev. D **86** (2012) 053014 [arXiv:1204.0445 [hep-ph]].

[12] S. F. King and C. Luhn, Rept. Prog. Phys. **76** (2013) 056201 [arXiv:1301.1340 [hep-ph]].

[13] S. F. King, A. Merle, S. Morisi, Y. Shimizu and M. Tanimoto, [arXiv:1402.4271 [hep-ph]].

[14] M. Tanimoto, AIP Conf. Proc. **1666** (2015) 120002.

[15] S. F. King, Prog. Part. Nucl. Phys. **94** (2017) 217 [arXiv:1701.04413 [hep-ph]].

[16] S. T. Petcov, Eur. Phys. J. C **78** (2018) no.9, 709 [arXiv:1711.10806 [hep-ph]].

[17] S. Pakvasa and H. Sugawara, Phys. Lett. **73B** (1978) 61.

[18] F. Wilczek and A. Zee, Phys. Lett. **70B** (1977) 418 Erratum: [Phys. Lett. **72B** (1978) 504].

[19] M. Fukugita, M. Tanimoto and T. Yanagida, Phys. Rev. D **57** (1998) 4429 [hep-ph/9709388].

[20] N. Haba, A. Watanabe and K. Yoshioka, Phys. Rev. Lett. **97** (2006) 041601 [hep-ph/0603116].

[21] E. Ma and G. Rajasekaran, Phys. Rev. D **64**, 113012 (2001) [arXiv:hep-ph/0106291].

[22] K. S. Babu, E. Ma and J. W. F. Valle, Phys. Lett. B **552**, 207 (2003) [arXiv:hep-ph/0206292].

[23] G. Altarelli and F. Feruglio, Nucl. Phys. B **720** (2005) 64 [hep-ph/0504165].

[24] G. Altarelli and F. Feruglio, Nucl. Phys. B **741** (2006) 215 [hep-ph/0512103].

[25] Y. Shimizu, M. Tanimoto and A. Watanabe, Prog. Theor. Phys. **126** (2011) 81 [arXiv:1105.2929 [hep-ph]].

[26] T. Morozumi, H. Okane, H. Sakamoto, Y. Shimizu, K. Takagi and H. Umeeda, Chin. Phys. C **42** (2018) no.2, 023102 [arXiv:1707.04028 [hep-ph]].

[27] S. K. Kang, Y. Shimizu, K. Takagi, S. Takahashi and M. Tanimoto, PTEP **2018** (2018) no.8, 083B01 [arXiv:1804.10468 [hep-ph]].

[28] H. Ishimori, Y. Shimizu, M. Tanimoto and A. Watanabe, Phys. Rev. D **83** (2011) 033004 [arXiv:1010.3805 [hep-ph]].

[29] F. Feruglio and A. Paris, JHEP **1103** (2011) 101 [arXiv:1101.0393 [hep-ph]].

[30] W. Grimus and L. Lavoura, JHEP **0809** (2008) 106 [arXiv:0809.0226 [hep-ph]].

[31] S. F. King, Phys. Lett. B **439** (1998) 350 [hep-ph/9806440].

[32] S. F. King, Nucl. Phys. B **562** (1999) 57 [hep-ph/9904210].

[33] G. C. Branco, R. Gonzalez Felipe, F. R. Joaquim and T. Yanagida, Phys. Lett. B **562** (2003) 265 [hep-ph/0212341].

[34] P. H. Frampton, S. L. Glashow and T. Yanagida, Phys. Lett. B **548** (2002) 119 [hep-ph/0208157].

[35] T. Endoh, S. Kaneko, S. K. Kang, T. Morozumi and M. Tanimoto, Phys. Rev. Lett. **89** (2002) 231601 [hep-ph/0209020].

[36] K. Bhattacharya, N. Sahu, U. Sarkar and S. K. Singh, Phys. Rev. D **74** (2006) 093001 [hep-ph/0607272].

[37] S. Goswami and A. Watanabe, Phys. Rev. D **79** (2009) 033004 [arXiv:0807.3438 [hep-ph]].

[38] S. F. Ge, H. J. He and F. R. Yin, JCAP **1005** (2010) 017 [arXiv:1001.0940 [hep-ph]].

[39] S. Goswami, S. Khan and A. Watanabe, Phys. Lett. B **693** (2010) 249 [arXiv:0811.4744 [hep-ph]].

[40] W. Rodejohann, M. Tanimoto and A. Watanabe, Phys. Lett. B **710** (2012) 636 [arXiv:1201.4936 [hep-ph]].

[41] K. Harigaya, M. Ibe and T. T. Yanagida, Phys. Rev. D **86** (2012) 013002 [arXiv:1205.2198 [hep-ph]].

[42] Y. Shimizu, R. Takahashi and M. Tanimoto, PTEP **2013** (2013) no.6, 063B02 [arXiv:1212.5913 [hep-ph]].

[43] J. Zhang and S. Zhou, JHEP **1509** (2015) 065 [arXiv:1505.04858 [hep-ph]].

[44] G. Bambhaniya, P. S. Bhupal Dev, S. Goswami, S. Khan and W. Rodejohann, Phys. Rev. D **95** (2017) no.9, 095016 [arXiv:1611.03827 [hep-ph]].

[45] T. Rink and K. Schmitz, JHEP **1703** (2017) 158 [arXiv:1611.05857 [hep-ph]].

[46] T. Rink, K. Schmitz and T. T. Yanagida, [arXiv:1612.08878 [hep-ph]].

[47] Y. Shimizu, K. Takagi and M. Tanimoto, JHEP **1711** (2017) 201 [arXiv:1709.02136 [hep-ph]].

[48] T. Morozumi, Y. Shimizu, H. Umeeda and A. Yuu, Phys. Lett. B **799** (2019) 135046 [arXiv:1905.11747 [hep-ph]].

[49] R. de Adelhart Toorop, F. Feruglio and C. Hagedorn, Nucl. Phys. B **858**, 437 (2012) [arXiv:1112.1340 [hep-ph]].

[50] F. Feruglio, [arXiv:1706.08749 [hep-ph]].

[51] J. C. Criado and F. Feruglio, SciPost Phys. **5** (2018) no.5, 042 [arXiv:1807.01125 [hep-ph]].

[52] T. Kobayashi, N. Omoto, Y. Shimizu, K. Takagi, M. Tanimoto and T. H. Tatsuishi, JHEP **1811** (2018) 196 [arXiv:1808.03012 [hep-ph]].

[53] T. Kobayashi, K. Tanaka and T. H. Tatsuishi, Phys. Rev. D **98** (2018) no.1, 016004 [arXiv:1803.10391 [hep-ph]].

[54] J. T. Penedo and S. T. Petcov, Nucl. Phys. B **939** (2019) 292 [arXiv:1806.11040 [hep-ph]].

[55] P. P. Novichkov, J. T. Penedo, S. T. Petcov and A. V. Titov, JHEP **1904** (2019) 174 [arXiv:1812.02158 [hep-ph]].

[56] T. Kobayashi and S. Tamba, Phys. Rev. D **99** (2019) no.4, 046001 [arXiv:1811.11384 [hep-th]].

[57] X. G. Liu and G. J. Ding, JHEP **1908** (2019) 134 [arXiv:1907.01488 [hep-ph]].

[58] R. C. Gunning, *Lectures on Modular Forms* (Princeton University Press, Princeton, NJ, 1962).

[59] P. P. Novichkov, J. T. Penedo, S. T. Petcov and A. V. Titov, JHEP **1904** (2019) 005 [arXiv:1811.04933 [hep-ph]].

[60] F. J. de Anda, S. F. King and E. Perdomo, Phys. Rev. D **101** (2020) no.1, 015028 [arXiv:1812.05620 [hep-ph]].

[61] H. Okada and M. Tanimoto, Phys. Lett. B **791** (2019) 54 [arXiv:1812.09677 [hep-ph]].

[62] T. Kobayashi, Y. Shimizu, K. Takagi, M. Tanimoto, T. H. Tatsuishi and H. Uchida, Phys. Lett. B **794**, 114 (2019) [arXiv:1812.11072 [hep-ph]].

[63] P. P. Novichkov, S. T. Petcov and M. Tanimoto, Phys. Lett. B **793** (2019) 247 [arXiv:1812.11289 [hep-ph]].

[64] G. J. Ding, S. F. King and X. G. Liu, Phys. Rev. D **100** (2019) no.11, 115005 [arXiv:1903.12588 [hep-ph]].

[65] T. Nomura and H. Okada, Phys. Lett. B **797**, 134799 (2019) [arXiv:1904.03937 [hep-ph]].

[66] P. P. Novichkov, J. T. Penedo, S. T. Petcov and A. V. Titov, JHEP **1907**, 165 (2019) [arXiv:1905.11970 [hep-ph]].

[67] H. Okada and M. Tanimoto, [arXiv:1905.13421 [hep-ph]].

[68] I. de Medeiros Varzielas, S. F. King and Y. L. Zhou, [arXiv:1906.02208 [hep-ph]].

[69] T. Nomura and H. Okada, [arXiv:1906.03927 [hep-ph]].

[70] T. Kobayashi, Y. Shimizu, K. Takagi, M. Tanimoto and T. H. Tatsuishi, [arXiv:1906.10341 [hep-ph]].

[71] H. Okada and Y. Orikasa, Phys. Rev. D **100** (2019) no.11, 115037 [arXiv:1907.04716 [hep-ph]].

[72] T. Kobayashi, Y. Shimizu, K. Takagi, M. Tanimoto and T. H. Tatsuishi, JHEP **2002** (2020) 097 [arXiv:1907.09141 [hep-ph]].

[73] G. J. Ding, S. F. King and X. G. Liu, JHEP **1909** (2019) 074 [arXiv:1907.11714 [hep-ph]].

[74] H. Okada and Y. Orikasa, [arXiv:1907.13520 [hep-ph]].

[75] S. F. King and Y. L. Zhou, Phys. Rev. D **101** (2020) no.1, 015001 [arXiv:1908.02770 [hep-ph]].

[76] T. Nomura, H. Okada and O. Popov, Phys. Lett. B **803** (2020) 135294 [arXiv:1908.07457 [hep-ph]].

[77] H. Okada and Y. Orikasa, [arXiv:1908.08409 [hep-ph]].

[78] J. C. Criado, F. Feruglio and S. J. D. King, JHEP **2002** (2020) 001 [arXiv:1908.11867 [hep-ph]].

[79] Gui-Jun Ding, S. F. King, X. G. Liu and J. N. Lu, JHEP **1912** (2019) 030 [arXiv:1910.03460 [hep-ph]].

[80] X. Wang and S. Zhou, [arXiv:1910.09473 [hep-ph]].

[81] T. Nomura, H. Okada and S. Patra, [arXiv:1912.00379 [hep-ph]].

[82] J. N. Lu, X. G. Liu and G. J. Ding, [arXiv:1912.07573 [hep-ph]].

[83] X. Wang, [arXiv:1912.13284 [hep-ph]].

[84] S. J. D. King and S. F. King, arXiv:2002.00969 [hep-ph].

[85] M. Abbas, arXiv:2002.01929 [hep-ph].

[86] N. Cabibbo, Phys. Rev. Lett. **10** (1963) 531.

[87] M. Kobayashi and T. Maskawa, Prog. Theor. Phys. **49** (1973) 652.

[88] Y. Fukuda *et al.* [Super-Kamiokande Collaboration], Phys. Rev. Lett. **81** (1998) 1562 [hep-ex/9807003].

[89] M. Tanabashi *et al.* [Particle Data Group], Phys. Rev. D **98** (2018) no.3, 030001.

[90] S. Weinberg, Phys. Rev. Lett. **43** (1979) 1566.

[91] P. Minkowski, Phys. Lett. B **67** (1977) 421; T. Yanagida, in Proceedings of the Workshop on Unified Theories and Baryon Number in the Universe, eds. O. Sawada and A. Sugamoto (KEK report 79-18, 1979); M. Gell-Mann, P. Ramond and R. Slansky, in Supergravity, eds. P. van Nieuwenhuizen and D.Z. Freedman (North Holland, Amsterdam, 1979); R. N. Mohapatra and G. Senjanovic, Phys. Rev. Lett. **44** (1980) 912; J. Schechter and J. W. F. Valle, Phys. Rev. D **22** (1980) 2227; J. Schechter and J. W. F. Valle, Phys. Rev. D **25** (1982) 774.

[92] C. Jarlskog, Phys. Rev. Lett. **55** (1985) 1039.

[93] P. F. Harrison, D. H. Perkins, W. G. Scott, Phys. Lett. B **530** (2002) 167 [arXiv:hep-ph/0202074].

[94] P. F. Harrison, W. G. Scott, Phys. Lett. B **535** (2002) 163-169 [arXiv:hep-ph/0203209].

[95] A. Gando *et al.* [KamLAND-Zen Collaboration], Phys. Rev. Lett. **117** (2016) no.8, 082503 Addendum: [Phys. Rev. Lett. **117** (2016) no.10, 109903] [arXiv:1605.02889 [hep-ex]].

[96] C. D. Froggatt and H. B. Nielsen, Nucl. Phys. B **147** (1979) 277.

[97] G. Altarelli, F. Feruglio and C. Hagedorn, JHEP **0803** (2008) 052 [arXiv:0802.0090 [hep-ph]].

[98] E. Giusarma, M. Gerbino, O. Mena, S. Vagnozzi, S. Ho and K. Freese, Phys. Rev. D **94** (2016) no.8, 083522 [arXiv:1605.04320 [astro-ph.CO]].

[99] S. Vagnozzi, E. Giusarma, O. Mena, K. Freese, M. Gerbino, S. Ho and M. Lattanzi, Phys. Rev. D **96** (2017) no.12, 123503 [arXiv:1701.08172 [astro-ph.CO]].

[100] N. Aghanim *et al.* [Planck Collaboration], [arXiv:1807.06209 [astro-ph.CO]].

[101] G. C. Branco, R. G. Felipe and F. R. Joaquim, Rev. Mod. Phys. **84** (2012) 515 [arXiv:1111.5332 [hep-ph]].

[102] G. Castelo-Branco and D. Emmanuel-Costa, Springer Proc. Phys. **161** (2015) 145 [arXiv:1402.4068 [hep-ph]].

[103] C. Patrignani *et al.* [Particle Data Group], Chin. Phys. C **40** (2016) no.10, 100001.

[104] Y. Shimizu, K. Takagi and M. Tanimoto, Phys. Lett. B **778** (2018) 6 [arXiv:1711.03863 [hep-ph]].

[105] T. Kobayashi, Y. Shimizu, K. Takagi, M. Tanimoto and T. H. Tatsuishi, Phys. Rev. D **100** (2019) no.11, 115045 [arXiv:1909.05139 [hep-ph]].

[106] T. Kobayashi, Y. Shimizu, K. Takagi, M. Tanimoto, T. H. Tatsuishi and H. Uchida, [arXiv:1910.11553 [hep-ph]].